THE EFFECT OF CALCITONIN GENE-RELATED PEPTIDE ON ACID-SENSING ION
CHANNEL ACTIVITY IN PRIMARY CELL CULTURE OF TRIGEMINAL GANGLION
NEURONS

Mr. Uggrit Junsre

A Thesis Submitted in Partial Fulfillment of the Requirements
for the Degree of Master of Science Program in Medical Science
Faculty of Medicine
Chulalongkorn University
Academic Year 2013
Copyright of Chulalongkorn University

ผลของแคลซิโทนินยีนรีเลทต์เปปไทด์ต่อการทำงานของเอซิดเซนซิ่งไอออนแชนแนล ในเซลล์
ประสาทเพาะเลี้ยงชนิดไตรเจมินัลแกงเกลี่ยนในระดับปฐมภูมิ

นายอุกกฤษฏ์ จันทร์ศรี

วิทยานิพนธ์นี้เป็นส่วนหนึ่งของการศึกษาตามหลักสูตรปริญญาวิทยาศาสตรมหาบัณฑิต
สาขาวิชาวิทยาศาสตร์การแพทย์
คณะแพทยศาสตร์ จุฬาลงกรณ์มหาวิทยาลัย
ปีการศึกษา 2556

Thesis Title	THE EFFECT OF CALCITONIN GENE-RELATED
	PEPTIDE ON ACID-SENSING ION CHANNEL
	ACTIVITY IN PRIMARY CELL CULTURE OF
	TRIGEMINAL GANGLION NEURONS
By	Mr. Uggrit Junsre
Field of Study	Medical Science
Thesis Advisor	ProfessorAnan Srikiatkhachorn, M.D.
Thesis Co-Advisor	Associate ProfessorSaknan Bongsebandhu-phubhakdi, Ph.D.

Accepted by the Faculty of Medicine, Chulalongkorn University in Partial Fulfillment of the Requirements for the Master's Degree

....Dean of the Faculty of Medicine

(Associate ProfessorSophon Napathorn, M.D.)

THESIS COMMITTEE

....Chairman

(ProfessorVilai Chentanez, M.D., Ph.D.)

....Thesis Advisor

(ProfessorAnan Srikiatkhachorn, M.D.)

....Thesis Co-Advisor

(Associate ProfessorSaknan Bongsebandhu-phubhakdi, Ph.D.)

....Examiner

(Assistant ProfessorNipan Israsena, M.D., Ph.D.)

....External Examiner

(Associate ProfessorBanthit Chetsawang, Ph.D.)

อุกกฤษฏ์ จันทร์ศรี : ผลของแคลซิโทนินยีนรีเลทต์เปปไทด์ต่อการทางานของเอซิดเซน ซิ่งไอออนแชนแนล ในเซลล์ประสาทเพาะเลี้ยงชนิดไตรเจมินัลแกงเกลี่ยนในระดับปฐม ภูมิ. (THE EFFECT OF CALCITONIN GENE-RELATED PEPTIDE ON ACID-SENSING ION CHANNEL ACTIVITY IN PRIMARY CELL CULTURE OF TRIGEMINAL GANGLION NEURONS) อ.ที่ปรึกษาวิทยานิพนธ์หลัก: ศ. นพ.อนันต์ ศรี เกียรติขจร, อ.ที่ปรึกษาวิทยานิพนธ์ร่วม: รศ. ดร.ศักนัน พงศ์พันธุ์ผู้ภักดี, 87 หน้า.

ภาวะความเป็นกรดเฉพาะบริเวณในภาวะของการอักเสบนำไปสู่การลดลงของค่าพีเอช และทำให้เกิดอาการปวดหัว โดยผ่านการทำงานของเซลล์ประสาทในปมประสาทไตรเจมินัลขนาด เล็กและกลาง เอซิดเซนซิ่งไอออนแชนแนลหรือเรียกเอซิคส์เป็นตัวรับรู้ความเป็นกรดที่ที่ซึ่ง ต้องการค่าพีเอชอย่างน้อยเจ็ดจุดศูนย์ที่ทำให้เกิดการหลั่งของสารสื่อประสาทชนิดต่างๆ รวมถึง แคลซิโทนินยีนรีเลทต์เปปไทด์ หรือเรียกซีจีอาร์พี ซึ่งซีจีอาร์พีสามารถกระตุ้นตัวรับของมันที่อยู่ที่ เซลล์ประสาทขนาดใหญ่ อย่างไรก็ตามบทบาทของซีจีอาร์พีต่อการทำงานของเอซิคส์ยังไม่เคยได้ ศึกษา นอกจากนี้บทบาทของพีเอชเจ็ดจุดศูนย์ต่อเซลล์ประสาทในปมประสาทไตรเจมินัลยังไม่ ชัดเจน การศึกษานี้มีวัตถุประสงค์เพื่อศึกษาผลของพีเอชเจ็ดจุดศูนย์ต่อเอซิคส์และเพื่อศึกษาผล ของซีจีอาร์พีซึ่งสามารถเปลี่ยนแปลงการทำงานของเอซิคส์ในทั้งเซลล์ประสาทขนาดเล็กถึงกลาง และเซลล์ประสาทขนาดใหญ่ ผู้วิจัยนำเซลล์ประสาทเพาะเลี้ยงชนิดไตรเจมินัลแกงเกลี่ยนในระดับ ปฐมภูมิ มาทำการทดลองโดยใช้วิธีการโฮลล์เซลล์แพชช์แคลมพ์ซึ่งให้ระดับกระแสไฟฟ้ากระตุ้นที่ เพิ่มขึ้นไปทางบวกในช่วงเวลาที่ยาวและสั้น คุณสมบัติทางไฟฟ้าของเซลล์ประสาทถูกเปรียบเทียบ ระหว่างค่าพีเอชปกติทางสรีรวิทยาและพีเอชเจ็ดจุดศูนย์ ทั้งในเงื่อนไขที่มีและไม่มีซีจีอาร์พี หลังจากลดค่าพีเอช พีเอชเจ็ดจุดศูนย์เพิ่มความตื่นตัวในเซลล์ประสาทขนาดเล็กถึงกลาง ขณะที่พี เอชเจ็ดจุดศูนย์ไม่สามารถเปลี่ยนแปลงความตื่นตัวในเซลล์ประสาทขนาดใหญ่ได้ นอกจากนี้ซีจี อาร์พีสามารถเพิ่มความตื่นตัวในเซลล์ประสาทขนาดใหญ่โดยผ่านการกระตุ้นที่ตัวรับของมัน อย่างไรก็ตามซีจีอาร์พีน่าจะเปลี่ยนแปลงความตื่นตัวในเซลล์ประสาทขนาดเล็กถึงกลางโดยผ่าน การแชทเทลไลท์เกลี่ยเซลล์ด้วยวิธีการที่ยังไม่รู้แต่น่าจะมีความเป็นไปได้ว่าเป็นกระบวนการแคส เคดด์สัญญาณ การค้นพบเหล่านี้บ่งบอกว่าค่าพีเอชเจ็ดจุดศูนย์สามารถเปลี่ยนแปลงความตื่นตัว ของเซลล์ประสาทขนาดเล็กถึงกลางและซีจีอาร์พียังสามารถเปลี่ยนแปลงความตื่นตัวของเซลล์ ประสาทขนาดใหญ่ได้ ซึ่งเป็นผลทำให้เกิดการรับรู้ความเจ็บปวด อย่างไรก็ตามผลของซีจีอาร์ต่อ การเปลี่ยนแปลงความตื่นตัวในพีเอชเจ็ดจุดศูนย์ของเซลล์ประสาทขนาดเล็กถึงกลางควรถูกศึกษา ต่อไป

สาขาวิชา	วิทยาศาสตร์การแพทย์	ลายมือชื่อนิสิต ....
ปีการศึกษา	2556	ลายมือชื่อ อ.ที่ปรึกษาวิทยานิพนธ์หลัก ....
		ลายมือชื่อ อ.ที่ปรึกษาวิทยานิพนธ์ร่วม ....

5374693830 : MAJOR MEDICAL SCIENCE

KEYWORDS: TRIGEMINAL GANGLION NEURONS / WHOLE CELL PATCH-CLAMP RECORDING / ASICS / CGRP / SMALL- TO MEDIUM-SIZED NEURONS / LARGE-SIZED NEURONS / EXCITABILITY

UGGRIT JUNSRE: THE EFFECT OF CALCITONIN GENE-RELATED PEPTIDE ON ACID-SENSING ION CHANNEL ACTIVITY IN PRIMARY CELL CULTURE OF TRIGEMINAL GANGLION NEURONS. ADVISOR: PROF.ANAN SRIKIATKHACHORN, M.D., CO-ADVISOR: ASSOC. PROF.SAKNAN BONGSEBANDHU-PHUBHAKDI, Ph.D., 87 pp.

The local tissue acidosis of inflammatory events leads to physiological pH drop and causes headache via the activation of small-to-medium-sized trigeminal ganglion (TG) neurons. Acid sensing ion channels (ASICs) are the acidic sensor in which requiring at least pH 7.0 to cause neurotransmitter release, such as CGRP. CGRP elevates nociceptive signal by activating its receptor on large-sized neurons. However, the role of CGRP on ASICs activity has not been investigated. Moreover, the role of pH 7.0 on TG neurons has still unclear. The present study aimed to investigate the effect of pH 7.0 on ASICs and to investigate whether the effect of CGRP can modulate ASICs activity in both the small-to-medium-sized and large-sized neurons. Primary-culture TG neurons were performed by whole-cell patch clamp recording that injected depolarizing current steps in long and short periods. The electrophysiological properties of neurons were compared between physiological pH and pH 7.0 in both with and without CGRP. After lowering pH, pH 7.0 increased the excitability in the small-to-medium-sized neurons while pH 7.0 cannot modulate the excitability in the large-sized neurons. Moreover, CGRP can directly increase the excitability in the large-sized neurons by activating its receptor. However, CGRP would modulate the excitability in the small-to-medium-sized neurons via the activation of satellite glia cells with unknown mechanism, but would possibly be the signaling cascade pathways. These finding indicate that pH 7.0 can modulate the excitability of small-to-medium-sized neurons and CGRP can directly modulate the excitability of large-sized neurons resulting in the increase of pain perception. However, the effect of CGRP to modulate the excitability in pH 7.0 should be further investigated.

Field of Study: Medical Science   Student's Signature ....

Academic Year: 2013   Advisor's Signature ....

Co-Advisor's Signature ....

ACKNOWLEDGEMENTS

CONTENTS

X

LIST OF TABLES

LIST OF FIGURES

Page

Page

LIST OF ABBREVIATIONS

μm	micrometer
AA	arachidonic acid
AC	adenylyl cyclase
AHP	afterhyperpolarization
AP	action potential
ASICs	acid-sensing ion channels
ATP	adenosine triphosphate
BBB	blood brain-barrier
BK	bradykinin
BK_{ca}	big conductance calcium-activated potassium channel
C	cervical
CaMKII	calcium/calmodulin-dependent protein kinase II
cAMP	cyclic adenosine monophosphate
CGRP	calcitonin gene-related peptide
CLR	calcitonin-like receptor
CNS	central nervous system
CREB	cAMP response element binding protein
CSD	cortical spreading depression
D	domain
DAG	diacylglycerol

ddH$_2$O	double distilled water
DRASIC	dorsal root acis-sensing ion channel
DRG	dorsal root ganglion
E$_m$	membrane potential
ENS	enteric nervous system
ER	endoplasmic reticulum
FMRF	phenylalanine-methionine-arginine-phenylalanine
FT	falling time
GTP	Guanine triphosphate
HBSS	hank's balanced salt solution
HP	holding potential
IL	interleukine
IFM	isoleucine, phenylalanine, and methionine
IP$_3$	inositol 1,4,5-trisphosphate
K2P	two pore domain potassium channel
K$_v$	voltage-gated potassium channel
MAPK	mitogen-activated protein kinase
MMP-9	matrix metalloproteinases 9
ms	millisecond
mV	millivolt
Na$_v$	voltage-gated sodium channel

NPFF	neuropepide phenylalanine -leucine-phenylalanine-glutamine-proline-glutamine-arginine- phenylalanine
NPSF	neuropepide serine-leucine-alanine-alanine-proline-glutamine-arginine-phenylalanine
NGF	nerve growth factor
NO	nitric oxide
NS	nociceptive specific
$P2X_3$	purinergic receptor P2X, ligand-gated ion channel 3
PDL	poly-D-lysine
PM	pore module
PGE_2	prostaglandin E2
PKA	protein kinase A
PKC	protein kinase C
PIP_2	phosphatidylinositol 4,5-biphosphate
PLC	phospholipase C
PNS	peripheral nervous system
RAMP1	receptor activity-modifying proteins 1
RCP	receptor component protein
RT	rising time
S	segment
SEM	standard error mean

SGC   satellite glia cell

SK_{ca} small conductance calcium-activated potassium channel

SP   substance P

SPASIC   spinal cord acid-sensing ion channel

SNAP-25   synaptosomal-associated protein of 25 kDa

TWIK   two pore domain potassium channel

TASK-3   TWIK-related acid sensitive K^+ channel 3

TCC   trigeminocerviacal complex

TG   trigeminal ganglion

TNC   trigeminal nucleus caudalis

TNF   tumor necrosis factor

TRESK   TWIK-related spinal cord K^+ channel

TRPV1   transient receptor potential vanilloid 1

VPM   ventromedial thalamic nucleus

VSD   voltage sensing domain

WDR   wide dynamic range

CHAPTER I

INTRODUCTION

Background and Rationale

The inflammatory events of trigeminal ganglion (TG) neurons associated with headache leading to an acidosis of local area is called 'local tissue acidosis' (1, 2). The levels of pH in the local tissue acidosis are decreased from physiological pH to pH 5.4 that can activate the specific receptors and nociceptors to produce headache (3, 4). These receptors are defined as acid-sensing ion channels (ASICs) and transient receptor potential vanilloid type 1 (TRPV1) that responds to pH in different ranges. ASICs activation requires pH change from 7.4 to 7.0, while TRPV1 activation requires the pH change less than 6.0. (5, 6). Thus, ASICs are the primary pH sensor in response to acidic noxious stimulus.

ASICs are the voltage-independent ligand-gated cation channels that assemble three subunits to form function. ASICs are activated by the extracellular proton (H^+), and then this activation results in permeability to sodium (Na^+) ions (7). ASICs are divided into ASIC1a, ASIC1b, ASIC2a, ASIC2b, ASIC3, and ASIC4 that distribute in many tissues in the central and peripheral nervous system (CNS and PNS) (8). In TG and dorsal root ganglion (DRG), ASIC1a and 3 distribute on small-to-medium-sized neurons, while ASIC3 distributes on large-sized neurons (9-11). Although small-to-medium-sized neurons implicate with nociceptor, large-sized neurons implicates on mechanoreceptor and proprioceptor (8, 12). In the range of pH, pH change from 7.4 to 7.0 sufficiently activates ASICs on the small-to-medium-sized neurons that can produce the excitability in DRG, nodose ganglion, and dural afferent part of TG (13-15). However, the physiological mechanism that pH 7.0 can increase the excitability in TG neurons is still unclear. Especially, the effect of pH 7.0 on the small-to-medium-sized and large-sized neurons should be investigated because the expression patterns of ASICs on them are difference.

ASICs co-express with other receptors, such as TRPV1, purinergic receptor (P2X), purinoceptor ligand-gated ion channel 3 ($P2X_3$). Moreover, ASICs co-express

with calcitonin gene-related peptide (CGRP) in the small- to-medium-sized neurons. The co-expression of ASICs and CGRP is thought to be the reason that makes TG neurons respond to low pH, capsaicin, and ATP stimuli (16-18). CGRP activation can sensitize $P2X_3$ that leads to prolonged headache, and CGRP can also up-regulate TRPV1 expression (19, 20). The modulation of CGRP on ASICs is unknown, albeit the activation of ASICs can modulate the release of CGRP from the small-to-medium-sized neurons (21).

CGRP, a 37 amino acid vasodilatory neuropeptide, is released from the small-to-medium-sized neurons. CGRP acts through the functional CGRP receptor to dilate vessel, activate mast cells and satellite glia cells (SGCs), and modulate the large-sized neurons (22). Mast cells activation leads to degranulation and release of the inflammatory mediators, and SGCs activation leads to release of the pro-inflammatory mediators (23). These mediators can activate, in turn, the small-to-medium-sized neurons (24). The implication between CGRP and ASICs was studied by the observation of co-expression. Both ASICs and CGRP are co-expressed in small-to-medium-sized neurons in DRG and TG (10, 11). When the extracellular proton activates ASICs on TG neurons, Na^+ influx occurs that results in the increase of intracellular Na^+. Then, the elevation of intracellular Na^+ promotes the release of CGRP (21). However, there is co-expression of CGRP and ASICs3 in large-sized TG neurons (10, 25). Thus, whether CGRP can modulate ASICs via its receptor should be investigated.

Research questions

How does low pH (pH 7.0) modulate the neuronal excitability of the small-to-medium-sized neurons? Does pH 7.0 have any effect on ASICs of the large-sized neurons? Does CGRP have any effect on ASICs activity of the small-to-medium-sized and large-sized neurons?

Objectives

1. To determine the effect of pH 7.0 on ASICs in the small-to-medium-sized neuron.

2. To investigate the effect of pH 7.0 on ASICs in the large-sized neurons.

3. To investigate the modulation of CGRP on ASICs activity in the small-to-medium-sized neurons.

4. To investigate the modulation of CGRP on ASICs activity in the large-sized neurons.

Hypothesis

ASICs activation increases the neuronal excitability in the small-to-medium-sized neurons, while CGRP modulation enhances the AP induction in the large-sized neurons.

CHAPTER II

LITERATURE REVIEWS

Trigeminal nociceptive system

Head and face are innervated by the trigeminal nerve, which is divided into three branches; ophthalmic (V1), maxillary (V2), and mandibular (V3) branches (26). First, the ophthalmic branch (V1) innervates frontal sinus, orbit and eye, tentorium cerebelli, anterior and middle cerebral arteries, and superior sagittal sinus. Second, the maxillary branch (V2) innervates upper jaw, nose, and maxillary sinus. Third, the mandibular branch (V3) innervates lower jaw, masticatory muscles, and temperomandibular joint (27). Moreover, three branches also give the fibers to supply dura mater of brain structures including dural and pial vessels (28). These branches emerge from their neurons in the trigeminal ganglion (TG) and continue to the brainstem and upper cervical levels.

Trigeminal ganglion neurons

TG neurons, the first-order neuron, are pseudounipolar and enveloped in satellite glia cells at their cell bodies (29, 30). On the basis of the morphological and histological differences, the body of the TG neurons are classified into large light neurons, medium light neurons, medium dark neurons, small light neurons, and small dark neurons (29, 31). However, the TG neurons are divided into small-sized (> 30 μm or > 600 μm^2), medium-sized (30-40 μm or 1200 μm^2), and large-sized (< 40 μm or < 1200μm^2) neurons by using the immunohistologically neurochemical markers, including calcitonin gene-related peptide (CGRP) and phosphorylated neurofilament heavy chain 200 kDa (NF200). Each size of neurons has unique fiber; the small-sized and medium-sized neurons are defined as a nociceptive phenotype, give the unmyelinated C-fiber and thinly myelinated A-delta fiber, respectively. Thought, the large-sized neuron is defined as a non-nociceptive phenotype, gives the thick myelinated A-beta fiber (17, 32, 33). The A-beta fibers respond to the innocuous touch and proprioception stimuli, while the A-delta fibers detect and C-fibers detect

the noxious heat mechanical, thermal, and chemical stimuli (34). Following the basis of the protein expression, the nociceptive phenotype neurons are sub-classified into the peptidergic which expresses CGRP and substance P, and non-peptidergic which expresses Ret protein and binding isolectin B_4 (12, 35). However, both the peptidergic and non-peptidergic subtypes can overlap between the co-localization of CGRP and IB_4 in the rat (36). Moreover, the TG neurons contain neuropeptide that concerning with size of neurons; small sized neurons contain substance P, CGRP, cholecystokinin, somatostatin, vasoactive intestinal polypeptide, and gelanin; medium size neurons contain CGRP and neuropeptide Y; and large-sized neurons contain cholecystokinin and neuropeptide Y (33).

Thus, phenotypes of TG neurons convey the non-nociceptive and nociceptive information from peripheral stimuli to central nervous system for interpreting the input information into pain perception.

Nociceptor and pain perception

Pain is an unpleasant perception and emotion through an interaction between mechanisms of a sensory and cognition, which in the midst of the inflammation, disease, or trauma. The results of pain lead to a suffering and an avoidance from threatening situations (37, 38). Threat or stimulus, which potentially damages the tissues is defined as 'noxious'. For example, the heat that elicits pain in animals and human is higher than 45 °C, and is defined as noxious heat stimulus. Moreover, noxious can also be mechanical and chemical stimuli. These noxious stimuli have receptors with high-threshold for activation, and called 'nociceptor' or 'nociception', which were defined by Charles Sherrington (1906). Primary trigeminal nociceptors including dorsal root ganglion (DRG) and trigeminal ganglion (TG) neurons send unmyelinated C-fibers and thinly myelinated A-delta fibers, specifically mediate pain via responding in the single of noxious stimulus or the several of noxious stimuli, in which defining as polymodal nociceptors (34, 39). The nociceptors has three functional roles that transduce peripheral terminal, and convert external stimuli into electrical impulses including action potential (AP), conduction of impulses (or AP)

that run along axon to cell body, transmission of central terminal that synapses on specific noceiceptive second order neurons in the central nervous system (CNS) (40). Moreover, the nociceptors also enable the sensitization by threshold reduction and response elevation to the noxious stimuli (39).

Under the inflammatory conditions associated with the pathophysiology of head pain (including temporomandibular disorder, facial pain and migraine), the tissue damage that leads to release of inflammatory mediators such as extracellular proton (H^+), bradykinin (BK), nitric oxide (NO), prostaglandins (PGE_2), nerve growth factor (NGF), and adenosine triphosphate (ATP) that activate nociceptors (2, 16, 41-44). Similarly, cortical spreading depression (CSD), a depolarizing wave that occurs during migraine attack also leads to release of inflammatory mediators including H^+, arachinodic acid (AA), NO, and potassium (K^+) from cerebral cortex to the extracellular fluid. CSD increases matrix metalloproteinases 9 (MMP-9) level to interrupt blood- brain barrier (BBB), and then activates the nociceptive afferent at pial and dural vessels (45, 46). These mediator stimuli are transduced by a transducer protein or various transducer proteins. For example, the extracellular H^+ activates acid sensing ion channels (ASICs) and/or transient receptor potential vanilloid 1 (TRPV1) that transduce signal to electrochemical impulses (47). The impulse is transmitted along the nociceptive axon and synapses on the neurons in the superficial layer (laminae I and II) that terminated by C-fiber, and the deeper layer (laminae III and IV) that are terminated by A-delta fiber, of the trigeminal nucleus caudalis (TNC) and C1-C3 spinal dorsal horn (48, 49). Moreover, the TNC and C1-C3 cervical cords are grouped and referred to the trigeminocerviacal complex (TCC) (50). The neurons in the TCC are classified into wide dynamic range (WDR) which respond to innocuous stimuli at deep layer, and nociceptive specific (NS) which respond to noxious stimulus, neurons that mainly locate at superficial layers (51, 52). The impulses from these neurons in the TCC give ascending fibers that decussate and convey information to the third-order neurons in the ventromedial thalamic nucleus (VPM) of thalamus and medial nucleus of the posterior group intralaminar complex via trigeminothalamic tract (or known as quintothalamic tract). The third-order neurons project thalamocortical axon to the facial region in the primary

somatosensory cortex that translate impulses into the perception of pain or headache (53).

In addition to CNS transmission, meanwhile, the nociceptors synthase vasoactive neuropeptides such as CGRP and substance P (SP) in the cell body and transport them to peripheral terminal. These neuropeptide cause the neurogenic inflammation and sensitization in head pain (54).

Neurogenic inflammation

Neurogenic inflammation is mediated by CGRP and SP. CGRP is proposed to play a role in the initiation of this inflammation (55, 56). In the peripheral afferent within high density of blood vessels, SP produces plasma protein extravasation, while CGRP produces vasodilation and mast cell degranulation (57-59). Moreover, CGRP also activates the satellite glia cells, which locate around trigeminal ganglion neurons (60). Both the mast cell degranulation and SGC activation lead the release of pro-inflammatory mediators and cytokines that contribute to the nociceptor sensitization (61). The mast cells locate near meningeal nociceptors and blood vessels, temporomadibular joint, buccal mucosa, toung, palate, as well as cutaneous tissues (62, 63). The activation of the mast cells by neuropeptides, especially CGRP, causes its degranulation that leads to release of histamine, bradykinin, nerve growth factor (NGF), serotonin, as well as the cytokines including, interleukin-1 (IL-1), IL-6, and tumor necrosis factor-alpha (TNF-alpha) resulting in nociceptors activation and enhancement of neuronal excitability (61-64). Moreover, the mast cell degranulation can produce a prolonged excitation in the nociceptors, especially C-fiber, that is long-lasting at least 4 hour and causes c-*fos* expression in TNC nociceptive neurons (65). In addition to the mast cells, SGC is another one in response to CGRP and causes neurogenic inflammation (23). SGC activation leads to release of TNF-alpha, IL-1beta, and prostaglandin E_2 (PGE_2), that activate the nociceptors and enhance neuronal excitability (24, 66). In summary, mast cells degranulation is an important process in the peripheral nociception, and SGCs activation is also an important

process in cell bodies sensitization that are involved in the development of peripheral sensitization (61).

Calcitonin gene-related peptide (CGRP) and its receptor

CGRP, a 37 amino acid vasodilatory neuropeptide, is a member of the calcitonin family, had been identified by Rosenfield in 1983. CGRP is classified into alpha-CGRP, which expresses in the nervous system (peripheral and central nervous system: PNS and CNS, respectively), and beta-CGRP, which expresses in the enteric nervous system (ENS) and pituitary gland. Alpha-CGRP and beta-CGRP isoforms are not difference in their biological activities, however, they differ in the sequence of amino acids (67). CGRP affects CGRP receptor that consists of calcitonin-like receptor (CLR), a seven-transmembrane G-protein-coupled receptor, interacting with receptor activity-modifying proteins 1 (RAMP1), a small single-transmembrane protein, and receptor component protein (RCP), an accessory protein (67). CLR require both RAMP1 and RCP to form a functional unit that RAMP1 transports CLR to plasma membrane as a mature glycoprotein and facilitates CGRP binding, while RCP directly binds to CLR, and facilitates the coupling of CGRP receptor to the intracellular signaling pathways (68, 69).

Distribution of CGRP and its receptor

CGRP and its receptor express in the nervous, cardiovascular, respiratory, and gastrointestinal systems (70, 71). In the peripheral nervous system (PNS), CGRP and its receptor are distributed in distinctive location. CGRP expresses on unmyelinated nerve fibers (defined as C-fibers) which are small-to-medium- sized neurons projecting to the spinal trigeminal region and superficial laminae (I and II) of the spinal trigeminal nucleus and C-1 of spinal cord level. In the other way, CGRP receptor (CLR+RAMP1) expresses on myelinated nerve fibers (defined as A-delta fibers) which are large-sized neurons, also projecting to the spinal trigeminal tract region and laminae I and II of the spinal trigeminal nucleus and C-1 of spinal cord

level. In addition to neurons, CGRP receptor, but not CGRP expresses on medial vascular smooth muscle layer, mast cells, and SGCs (72-74). Moreover, CGRP is co-expressed with synaptosomal-associated protein of 25 kDa (SNAP-25) in all regions of C-fiber neurons that SNAP-25 facilitates CGRP vesicle trafficking and CGRP secretion resulting in a paracrine signaling manner to activate blood vessels, mast cells, SGCs, and A-delta fibers (25, 75). Generally, CGRP and its receptor are not co-localized in the same neurons, however there is rare case that they are co-localized as auto-receptor (interaction with CGRP and its receptor in the same neurons) (25, 76). Thus, CGRP acts as a mediator in the intraganglionic communication between neurons and non-neuronal cells for neurogenic inflammation and peripheral sensitization as well as for relaying nociceptive information to higher-order neurons in brain (22, 77).

CGRP receptor-mediated signal transduction and peripheral sensitization

In the trigeminal nociception, the activation of CGRP receptor is induced by CGRP that couples to the intracellular signaling cascade and phosphorylates ion channels via protein kinase A (PKA), PKC, Ca^{2+}/ calmodulin-dependent kinases II (CaMKII) and mitogen-activated protein kinase (MAPK) pathways.

In the PKA pathway, the CGRP receptor activation couples to the signal transduction via $G_{alpha-s}$ protein that is commonly affected in neural function. The actived $G_{alpha-s}$ protein stimulates adenylyl cyclase (AC) that produces cyclic adenosine monophosphate (cAMP) resulting in PKA activation (69). The targets of PKA activation are ion channels and cAMP response element binding protein (CREB) that involves in physiological and neuronal effects. The vasodilation occurs under the activation of CGRP receptor on vascular smooth muscle cells via cAMP and PKA stimulation (78). Moreover, PKA is the important signal in the regulation of auto-activated receptor that it enhances CGRP promoter activity and then results in transcribing CGRP mRNA. This causes CGRP self-regulated sensitization and auto-regulation is upon on the expression of RAMP1 (79). The effect of CGRP on an ion channels has been studied in P2X$_3$ receptor. CGRP activated P2X$_3$ receptor trafficking via PKA. P2X$_3$ receptor is phosphorylated and translocated from the intracellular

stores to the surface of neuronal membrane (19). Moreover, PKA phosphorylates CREB, a gene regulatory protein that results in increase of $P2X_3$ mRNA expression (80). Thus, CGRP sensitizes the trigeminal ganglion neurons via PKA pathways.

In the PKC and CaMKII pathways, the signal transduction is mediated by $G_{alpha-q/11}$ protein which activates the phospholipase C-beta (PLC-beta) to hydrolyze phosphatidylinositol 4,5-biphosphate (PIP_2) into inositol 1,4,5-trisphosphate (IP_3) and diacylglycerol (DAG). IP_3 bind to IP_3-gated Ca^{2+}-release channel (IP_3 receptor) on endoplasmic reticulum (ER) which releases Ca^{2+} into the cytoplasm, whereas DAG modulate intracellular Ca^{2+} which activates the PKC, and PKC further phosphorylates ion channels (81, 82). PKC also phosphorylates and inserts $P2X_3$ receptor from the cytoplasm to the membrane surface (19). Moreover, intracellular Ca^{2+} binds to calmodulin, and activates Ca^{2+}/ calmodulin-dependent kinases II (CaMKII), and then CaMKII phosphorylates CREB and increase $P2X_3$ mRNA (80). These suggest that CGRP increases the intracellular Ca^{2+} via $G_{alpha-q/11}$ protein and sensitize $P2X_3$ receptor via PKC and CaMKII.

MAPK cascades including ERK, JNK, and p38 expression, are up-regulated by CGRP that activates CGRP receptor on SGCs (83, 84). SGCs release cytokines that activate TG neurons causing the peripheral sensitization (23). However, the mechanism whether CGRP receptor couples MAPK signaling is still unclear. It may be depended on whether G_{alpha} or other mechanisms (82).

In summary, the activation of CGRP receptor produces strong and prolonged pain that causes peripheral sensitization via the phosphorylation of ion channels and target proteins by PKA, PKC, CaMKII and MAPK (44, 83). Thus, CGRP sensitizes receptor or ion channel via the intracellular signaling pathway that leads to prolonged headache. However, the relationship between CGRP and ASICs are still unexplored.

Acid-sensing ion channels (ASICs)

The inflammatory events associated with the pathophysiology of head pain and lead to a local tissue acidosis. The high concentrations of proton (H^+) can reduce

pH value from physiological pH (pH 7.4) to pH 5.4 (3). Pain is evoked by extracellular H^+ that opens cation channel in nociceptors (1, 4). The receptors of extracellular H^+ are acid-sensing ion channels (ASICs) and transient receptor potential vanilloid type 1 (TRPV1), and they have different sensitivity to pH values (34). In the aspect of sensitivity to pH change, ASICs are more sensitive than TRPV1. ASICs require pH change only from pH 7.4 to pH 7.0 for its activation, while TRPV1 requires pH change from pH 7.4 to pH 6.0 (5, 6). Thus, ASICs are main sensor to detect acidic noxious in the tissue acidosis.

ASICs, which had been cloned by the Waldmann and colleague, are trimeric voltage-independent ligand-gated cation channels and mainly permeable to sodium ions (Na^+) (7, 85). The structure of one subunit (monomeric) of ASICs consists of two hydrophobic transmembrane domains, intracellular N- and C-termini, and large extracellular loop with the conservative of cysteine-rich (86). There are six ASICs that consist of ASIC1 which is spliced into ASIC1a (85, 87) and 1b (9, 88), ASIC2 which is also spliced into ASIC2a (89, 90) and 2b (91), ASIC3 (dorsal root ASIC or DRASIC) (92), and ASIC4 (spinal cord ASIC or SPASIC) (93). However, ASIC4 is excluded, because it cannot function as H^+-gated cation channels (93).

The distribution of ASICs in nervous system

ASICs widely express on neurons in both central and peripheral nervous system (CNS and PNS). In the CNS, ASIC1a, 2a and 2b express in whole brain including the cerebral cortex, cerebellum, hippocampal formation, amygdaloid nuclei, hypothalamus, and basal ganglia, whereas, in the PNS, ASIC1a, 1b, 2b, and 3 are expressed on sensory neurons (9, 85, 89-92, 94). In TG, there are the expression of both ASIC1a and 3 which are specific on individual size of neurons. ASIC1a and 3 express on small-to-medium-sized neurons, and respond to noxious stimuli, while ASIC3 is also expressed on large-sized neurons, and have mechanoreceptor and proprioceptor properties (9-11, 16).

Biophysical properties of ASICs

The distinct properties of ASICs are dependent on assembly of 3 subunit compositions that forms homomultimeric or heteromultimeric channels. ASICs have permeability to $Na^+ > Ca^{2+} > K^+$, however, the selective permeability is various depending on types of ASICs. For example, ASIC1a has permeability to Na^+ and Ca^{2+}, while ASIC1b has not any permeability to Ca^{2+} (88, 95).

The pH sensitivity of ASICs is obtained from the values of the half-maximal activation ($pH_{0.5}$), is 5.8-6.8, 6.1-6.2, 4.5-4.9, and 6.4-6.6 for ASIC1a, 1b, 2a, and 3 homomultimeric channels, respectively (96, 97). However, ASIC2b cannot form homomultimeric channel function by itself. In acid-evoked current, ASICs generate transient inward current, which followed by rapidly desensitization that is sustained current in which occurring after the desensitization is almost completed. The order of time constant for desensitization is ASIC2a > ASIC1b > ASIC1a > ASIC3, while the order of percentage from sustained current to peak current is ASIC3 >> ASIC2a > ASIC1b > ASIC1a (97). These correlate to the shape of ASICs current. Moreover, ASIC3 is the important channel for displaying a sustained pain. ASIC3 responds the slightly continuous drop pH to pH 4.0 that generates only sustained current and produces the long-lasting sensation of pain (1, 92). ASICs transduce the chemical signal to electrical signal for transmission that associates with action potentials (APs). APs which elicited by pH change, are induced during transient inward current. This suggests that Na^+ influx through ASICs play the major role in producing APs (14).

Neuropeptides modulate ASICs

The neuropeptides which modulate ASIC1 and 3 in dorsal root ganglion (DRG) neurons are Phe-Met-Arg-Phe (FMRF)amide, neuropepide SF (Ser-Leu-Ala-Ala-Pro-Gln-Arg-Phe-amide, NPSF), and neuropepide FF (Phe-Leu-Phe-Gln-Pro-Gln-Arg-Phe-amide, NPFF) (98). These neuropeptides directly activate ASIC1 and 3 that ASIC3 is a major response resulting in an increase of peak amplitude of transient inward current, an increase of time constant of desensitization, and an induction of sustained current (99-102). Moreover, these neuropeptides also modulate ASIC1 and ASIC3 that

increase the neuronal excitability under the acidosis of inflammation (101). Thus, FMRFamide, NPSF, and NPFF modulate ASICs to produce the excitability of nociceptors under the inflammatory events. However, the other neuropeptides including SP and CGRP do not effect on ASICs mRNAs level (103). Moreover, the effect of SP and CGRP on ASICs properties is unclear and should be clarified in the future.

The relationship of ASICs and CGRP

The implication between ASICs and CGRP has been studied by the aspects of localization and modulation. In the study of localization, it has been revealed that ASICs and CGRP are co-expressed on small-to-medium-sized neurons in DRG and TG (10, 11). When the extracellular H^+ activates ASICs on TG neurons, Na^+ will fluxes into neurons that increase the levels of intracellular Na^+. The elevation of intracellular Na^+ promotes the release of CGRP (21). However, the co-expression of CGRP receptor and ASICs are unknown. Indeed, CGRP receptor expresses on large-sized TG neurons that is similar to ASIC3 (10, 25). Because of the difference in pattern expression, the effect of CGRP on ASICs in TG neurons may differ depending on cell phenotype.

Conceptual framework
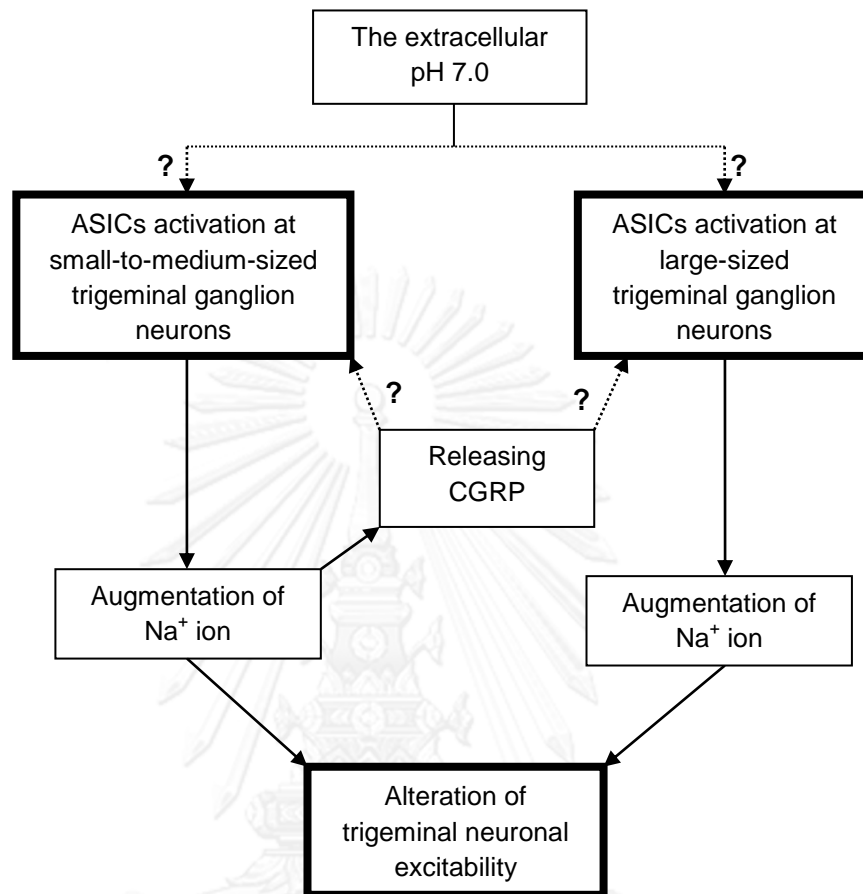
Figure 2.1 Conceptual framework

CHAPTER III

MATERIALS AND METHODS

MATERIALS

1. Chemicals

Adenosine 5′-triphosphate magnesium salt (Mg-ATP)	Sigma-Aldrich, MO, USA
Calcium chloride ($CaCl_2$)	Merck, Germany
Ethylenglycol-bis-(2-aminoethylethyl)-tetraacetic acid (EGTA)	Sigma-Aldrich, MO, USA
Glucose	Sigma-Aldrich, MO, USA
Guanosine 5′-triphosphate sodium salt hydrate (Na-GTP)	Sigma-Aldrich, MO, USA
HEPES free acid	Sigma-Aldrich, MO, USA
Laminin	Sigma-Aldrich, MO, USA
Magnesium chloride ($MgCl_2$)	Sigma-Aldrich, MO, USA
Poly-d-lysine (PDL) hydrobromide	Sigma-Aldrich, MO, USA
Potassium chloride (KCl)	Sigma-Aldrich, MO, USA
Potassium gluconate (K-gluconate)	Sigma-Aldrich, MO, USA
Potassium hydroxide (KOH)	Merck, Germany

Sodium chloride (NaCl)	Sigma-Aldrich, MO, USA
Sodium hydroxide (NaOH)	Merck, Germany

2. Drugs

Alpha-calcitonin gene-related peptide (alpha-CGRP)	Sigma-Aldrich, MO, USA
Sodium pentobarbital	Ceva Sante Animale, Libourne, France

3. Media

Collagenase type IV	Invitrogen, Carlsbad, CA, USA
Dispase II	Invitrogen, Carlsbad, CA, USA
Fetal bovine serum (FBS)	Gibco, Grand Island, NY, USA
Glutamax	Gibco, Grand Island, NY, USA
Ham's F-12	Gibco, Grand Island, NY, USA
Hank's balanced salt solution (HBSS)	Gibco, Grand Island, NY, USA
Leibovitz's L-15 medium (L-15)	Gibco, Grand Island, NY, USA
Papain	Sigma-Aldrich, MO, USA
Penicillin (10000 U/ml)/ Streptomycin (10000 µg/ml)	Gibco, Grand Island, NY, USA

4. Materials

Borosilicate glass pipettes

(1.5 mm OD × 0.86 mm ID)   Sutter Instruments, Navato, CA, USA

Calibrate graticule   Pyser, Kent, UK

Glass pasteur pipette   BRAND, Wertheim, Germany

   35 m × 10 mm dish   Corning, NY, USA

5. Instrumental devices

Bravia LCD TV BX300   Sony Thai Co., Ltd, Thailand

BX51WI fixed-stage upright

microscope   Olympus Corporation, Japan

CelCulture CO_2 incubator   Esco Global, Singapore

Class II biological safety cabinet

 model AC2   Esco Global, Singapore

Digitdata 1440 series interface   Axon Instruments, Foster City, CA, USA

Flaming/Brown micropipette

puller (P-97)   Sutter Instruments, Navato, CA, USA

Fiske® 210 Micro-osmometer   Advanced Instruments, Inc., MA, USA

High output vacuum/pressure

pump   EMD Millipore Corporation, MA, USA

MP-385-2 Micromanipulator   Sutter Instruments, Navato, CA, USA

Narishige MF-830 microforge   Narishige, Japan

Patch clamp amplifier:

Axopatch 200B	Axon Instruments, Foster City, CA, USA
Peristaltic pump: Minipuls 3	Gilson, S.A.S., Villiers le Bel, France
Rotina 420 R	Hettich Instruments, Bäch, Switzerland

Software for data acquisition:

Clampex 10.2	Axon Instruments, Foster City, CA, USA

Software for data analysis:

pClampfit 10.2	Axon Instruments, Foster City, CA, USA
Super HAD CCD II camera	Sony Corporation, Japan
Vibration isolation platform	Newport Corporation, CA, USA

EXPERIMENTAL DESIGN

The aim of this study is to determine the effect of pH 7.0 on ASICs in small-to-medium-sized and large-sized neurons. Moreover, we aim to investigate the modulation of CGRP on ASICs activity in small-to-medium-sized neurons and large-sized neurons. Thus, the experiments were separated into 2 major parts as described below.

1. Experiment I

The effect of pH 7.0 on phenotypes of trigeminal ganglion neurons was studied by using whole-cell patch-clamp configuration. The experiment was *in vitro* study. TG neurons were divided into 2 groups; small-to-medium-sized (n = 19) and large-sized neurons (n = 6). Both groups of neurons were superfused by the 2 types of extracellular solution that were physiological pH (pH 7.4) and low pH (pH 7.0). The extracellular solution was changed from pH 7.4 to pH 7.0 within 10 minutes. After lowering pH, the variables of the neuronal properties and AP shapes were measured and compared within their groups.
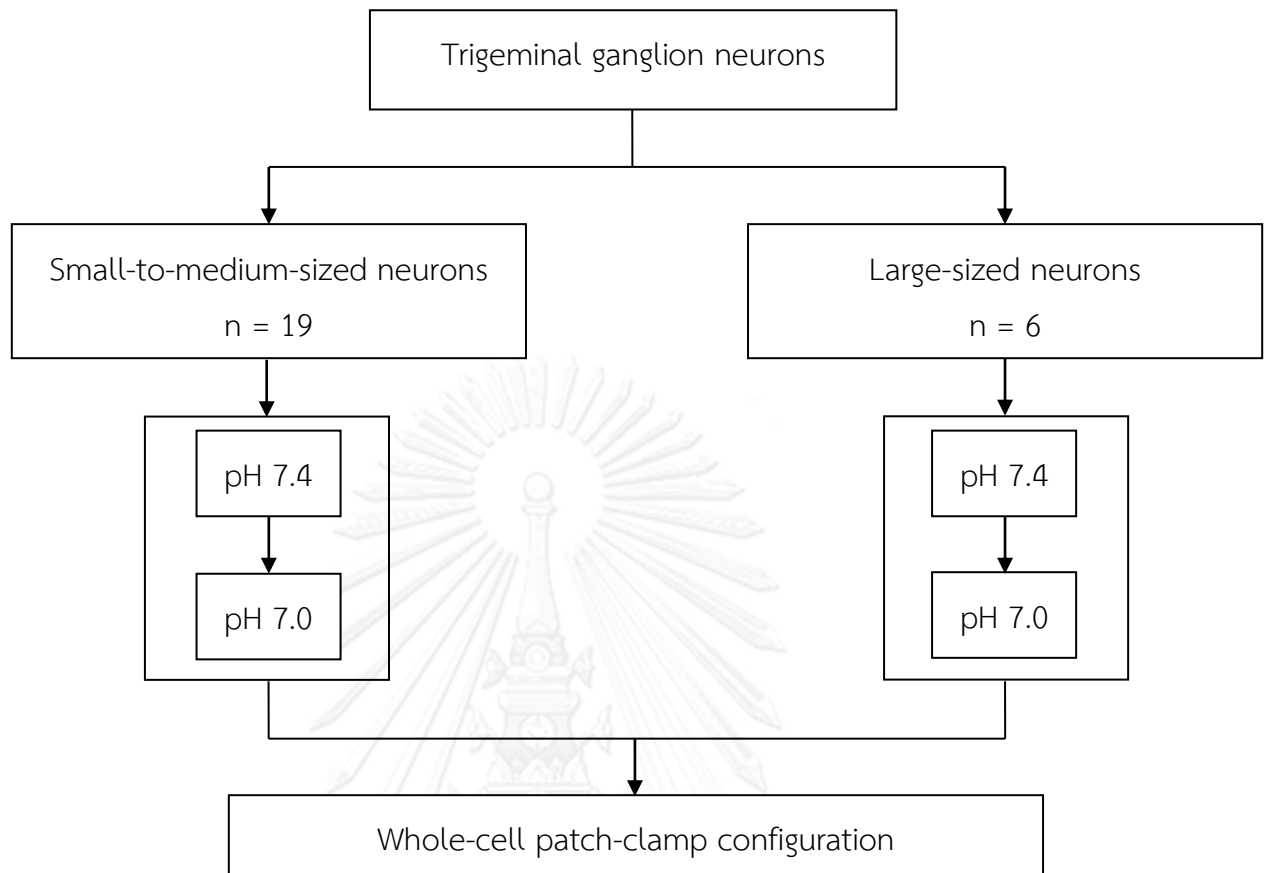
Figure 3.1 Diagram of experimental design of the experiment I.

2. Experiment II

The effect of CGRP on ASICs on phenotypes of trigeminal ganglion neurons was studied by using whole-cell patch-clamp configuration. The experiment was *in vitro* study. The experiment was *in vitro* study. TG neurons were divided into 2 groups; small-to-medium-sized (n = 9) and large-sized neurons (n = 6). Before recording, both groups of neurons were incubated with 1 μM CGRP in pH 7.4 for 1 hour at the room temperature. Next, the extracellular solution was changed to pH 7.0 with 1 μM CGRP that incubated for 10 minutes at the room temperature. The variables of the neuronal properties and AP shapes were measured and compared within in their groups.
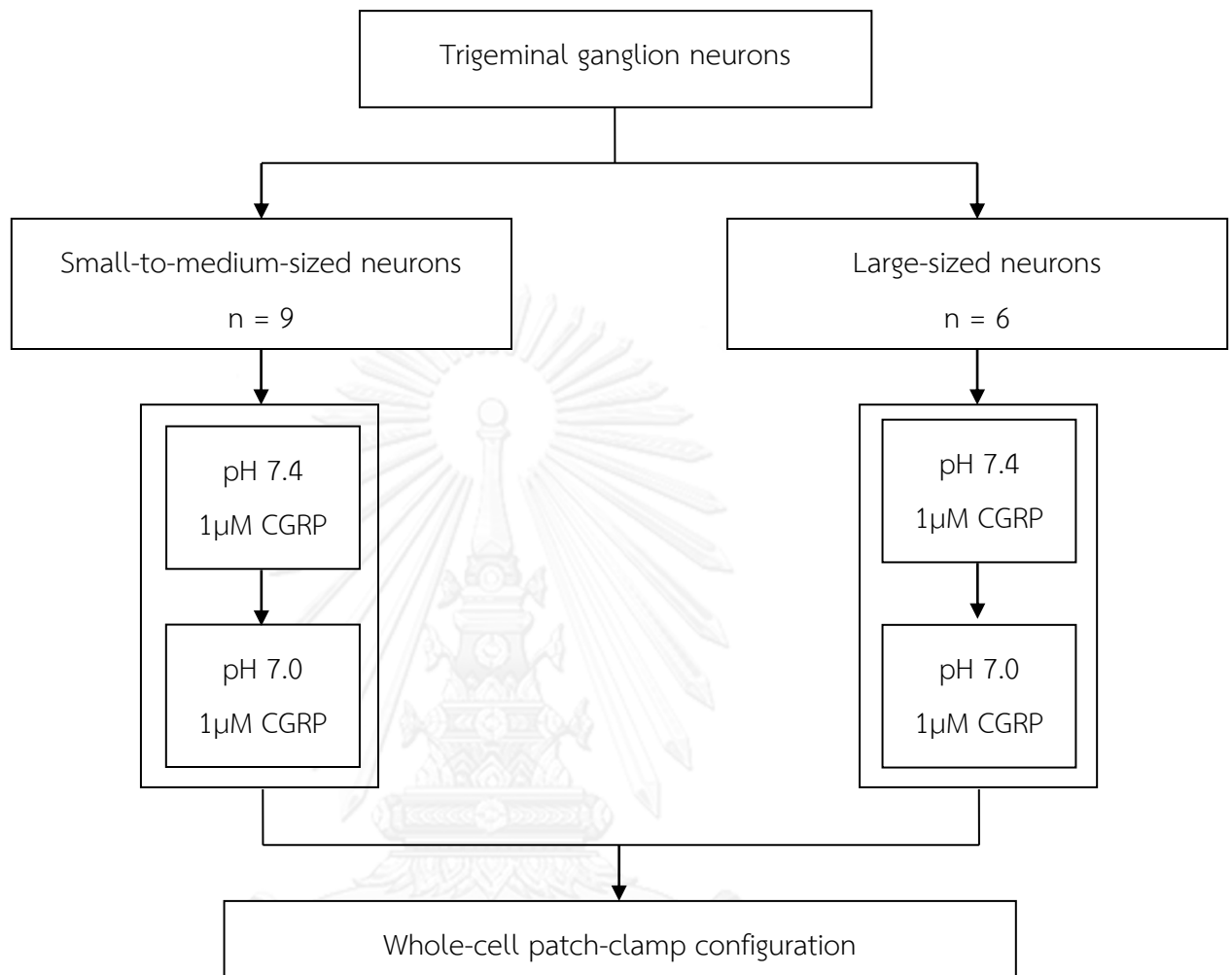
Figure 3.2 Diagram of the experimental design of the experiment II.

METHODS

1. Animals

Adult male Wistar rats were purchased from the National Laboratory Animal Center (Mahidol University, Salaya, Nakhonpathom, Thailand). Rats were maintained in a ventilated room on a 12 h dark/light cycle with free access to food and water in accordance with procedures approved by the Animal Care and Use Committee (Faculty of Medicine, Chulalongkorn University, Bangkok, Thailand).

2. Primary Culture

Trigeminal ganglion (TG) neurons were obtained from 4- to 8-week-old rats using a previously described dissociation protocol (104) with minor modifications as follows. Rats were euthanized by intraperitoneal injection of an overdose of sodium pentobarbital (Ceva Sante Animale, Libourne, France) and decapitated. Trigeminal ganglia were excised and transferred to a Petri dish containing ice-cold Hank's balanced salt solution without Ca^{2+}/Mg^{2+} (HBSS, Gibco, Grand Island, NY) and chopped into small pieces. After digestion in HBSS containing 10 mg ml^{-1} collagenase type IV (Invitrogen, Carlsbad, CA) and 18.2 U ml^{-1} dispase type II (Invitrogen) for 20 minutes at 37 °C followed by HBSS containing 1.5 mg papain (Sigma, St. Louis, MO) for 20 minutes at 37 °C, pieces of ganglia were triturated by passing them through sterilized fire-polished Pasteur pipette in L-15 medium (Gibco) containing 4.8% fetal bovine serum (FBS, Gibco), 10,000 units ml^{-1} of penicillin and 10,000 μg ml^{-1} of streptomycin (Gibco) and 1 M HEPES (Sigma). Dissociated neurons were spun at 1000 rpm to sediment the neurons. The neuronal cell pellet was resuspended in Ham's F-12 (Invitrogen) containing 10% FBS, 10,000 units ml^{-1} of penicillin and 10,000 μg ml^{-1} of streptomycin, and Glutamax (Gibco), and then plated onto 35 mm Petri dishes precoated with poly-d-lysine (PDL, Sigma) and laminin (Sigma). Neurons were maintained in an incubator at 37 °C under an atmosphere of 5% CO_2 and used within 24–48 h after plating.

Soma diameters, were classified into small (<30 μm), medium (30–40 μm), and large (>40 μm) diameter neurons shown in **Figure3.3**, as measured using a calibrated graticule (Pyser, Kent, UK) before whole-cell patch-clamp recordings.

Figure 3.3 Representative neurons, small-sized (23.40 μm, **A**), medium-sized (35.25 μm, **B**) and large-sized neurons (41 μm, **C**). These neurons were measured using a 40✕ objective lens. Scale bars all 10 μm.

3. Electrophysiological recording

Neurons were superfused at flow rate 2 ml min^{-1} with an extracellular solution containing 145 mM NaCl, 5 mM KCl, 2 mM $CaCl_2$, 1 mM $MgCl_2$, 10 mM d-Glucose, and 10 mM HEPES, pH 7.4 (adjusted with NaOH) and whole-cell patch-clamp recording was performed using an Axopatch 200B amplifier (Axon instruments, Foster City, CA) and pClamp 10 acquisition software (Axon instrument, City, ST). Borosilicate glass pipettes (1.5 mm OD × 0.86 mm ID, Sutter Instruments, Navato, CA) were pulled by using a Flaming–Brown micropipette puller (P-97, Sutter Instruments) and had resistance of 2–5 MΩ when polished with microforge (MF-830, Narishige, Japan) and filled with an internal solution containing 140 mM K-gluconate, 1 mM $CaCl_2$, 2 mM $MgCl_2$, 10 mM EGTA, 10 mM HEPES, 0.3 mM Na-GTP, and 10 mM Mg-ATP, pH 7.3 (adjusted with KOH). Neurons were voltage clamped at -60 mV and current was filtered at 5 kHz (using a low-pass filter) and sampled 25 kHz by using a Digidata 1440 series interface (Axon instruments). After whole-cell voltage clamp was established, the clamp switched to current clamp mode, which measured the resting membrane potential (RMP) with no applied current. Following and adapting a protocol described previously (105), applying short (1 ms) and long (500 ms)

depolarizing current pulses with -65 mV of holding potential (HP), to assess the action potential shape and the excitability of neurons, respectively. After recording in the extracellular solution at physiological pH (pH 7.4), to evaluate the effect of low pH, the extracellular solution was changed to pH 7.0. The time to change the solution was approximately 10 minutes.

The effect of CGRP on ASICs was evaluated, we dissolved alpha-CGRP (Sigma) in double-distilled water (ddH$_2$O) and added the alpha-CGRP solution to the extracellular solution at both pH 7.4 and 7.0 such that the final concentration of CGRP in each solution was 1 µM, as described in the previous study (19).

4. Action potential parameter assessments

When applying the 500 ms of current to define the excitability of neuron, threshold and rheobase were measured. Threshold was considered as the depolarizing potential that triggered the first AP (black dot, **Figure 3.4**) while the rheobase was the lowest injecting current that produced an AP (arrow**, Figure 3.4**). Total spikes was the number of spikes that triggered by depolarizing step currents from the 5th to 21st steps with increasing 5 pA per step.

A brief (1 ms) current was injected to assess the AP shape (**Figure 3.5**). AP height (AP$_{height}$) was measured from the membrane potential (E$_m$) to the peak of the AP, while AP overshoot (AP$_{overshoot}$) was measured at 0 mV to the peak of the AP. AP rising time (AP$_{RT}$) was measured from the threshold to the peak of the AP and the AP falling time (AP$_{FT}$) was measured from the peak to the E$_m$, whereas AP duration (AP$_{duration}$) was the sum of the rising and falling times (**Figure 3.5**). The depth of after-hyperpolarization (AHP$_{depth}$) was determined from the E$_m$ to the peak of the AHP, while the duration of the AHP was measured from the peak of the AHP to 50% of recovery to the baseline (AHP$_{50}$) (**Figure 3.6**).
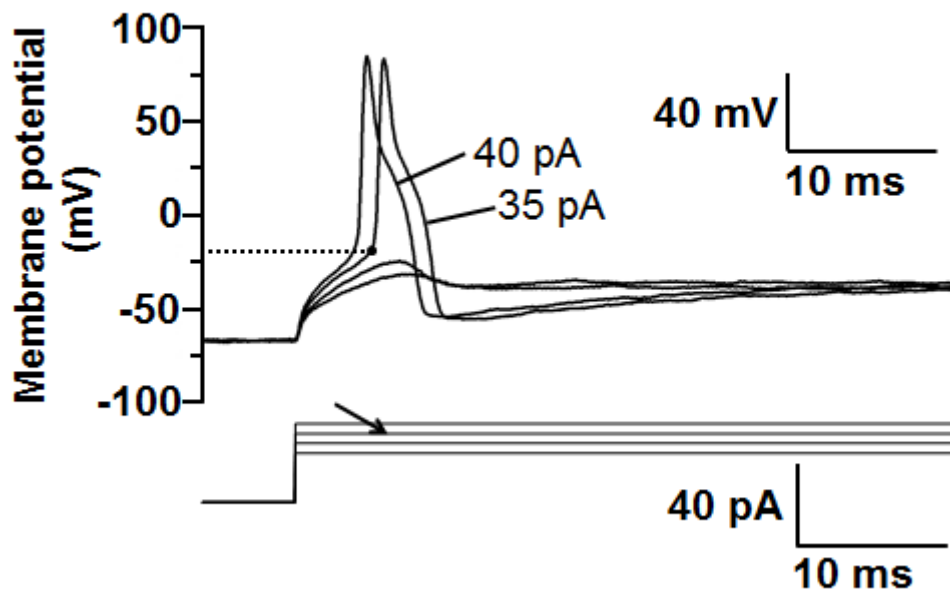
Figure 3.4 Measurement of threshold and rheobase. Upper: Threshold was measured at black dot with value as -21.63 mV, while rheobase was measured at first spike with value of 35 pA. Lower: The depolarizing current steps were injected to evoke the action potential, which first spike was evoked by the 11th step with value of 35 pA (arrow).
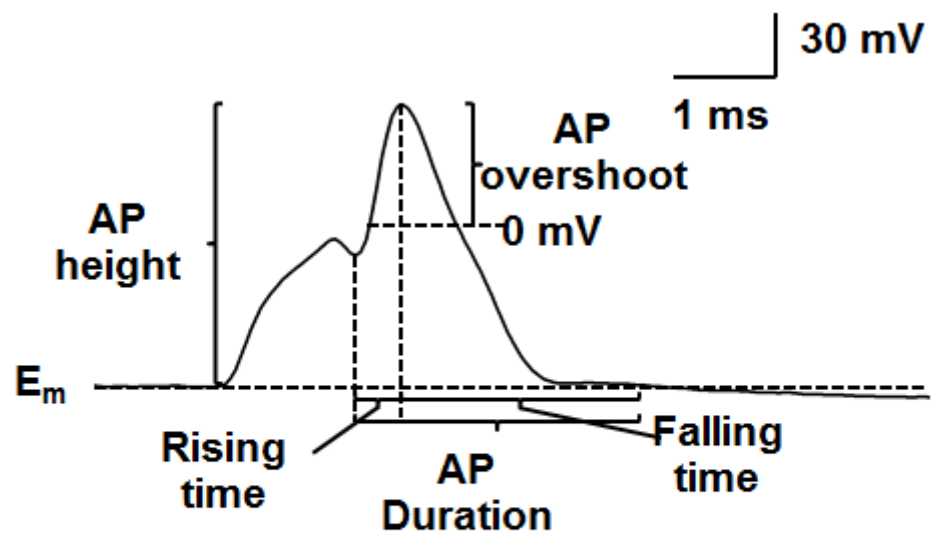
Figure 3.5 The illustration shows that the action potential (AP) parameters were assessed by injected 1ms current. The AP parameters; height, overshoot, rising time, falling time, and duration were recorded. E_m was membrane potential.
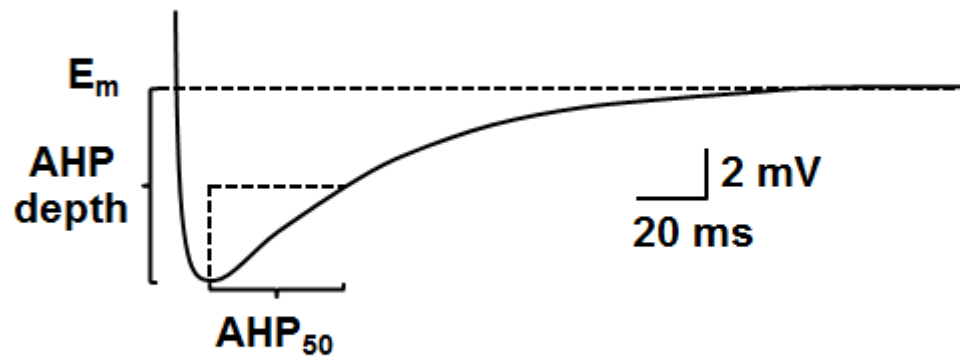
Figure 3.6 The illustration shows that the after-hyperpolarizaiton (AHP) parameters was assessed with depth of AHP and duration at half of recovery to baseline of AHP (AHP$_{50}$). E$_m$ was membrane potential.

5. Data analysis

All data are presented as mean ± standard errors of means (SEM). Statistical analysis was performed using Student's *t* test (Sigma Plot version 10.0, City, State, USA). $P < 0.05$ was accepted as statistically significant.

CHAPTER IV

RESULTS

Effect of pH 7.0 on the small-to-medium-sized TG neurons

Depolarizing current pulses with 500 ms were applied to small-to-medium-sized neurons (<40 μm; n = 19) before and after decreasing the pH from physiological (pH 7.4) to pH 7.0 as shown in representative trace (**Figure 4.1**). The RMP was significantly depolarized at pH 7.0 (**Figure 4.2** and **Table 4.1**). Small-to-medium-sized neurons tended to produce more spikes, but this change was not significant compared to control (**Figure 4.3**). Totally, small-to-medium-sized neurons were excited in response to low pH (**Table 4.1**). Their threshold was significantly shifted to more negative at pH 7.0 (**Figure 4.4**) and rheobase was significantly decreased (**Figure 4.5**).

Action potential (AP) shapes and variables were measured by applying a 1 ms depolarizing current pulse (**Table 4.1**). The AP_{height} at physiological pH was significantly smaller than control at pH 7.0 (**Figure 4.6**), and the $AP_{overshoot}$ was also significantly smaller than control (**Figure 4.7**). The magnitude of the AHP_{depth} of the neurons was significantly decreased at pH 7.0 (**Figure 4.8**), while the AHP_{50} was significantly longer than control at pH 7.0 (**Figure 4.9**). However, there were no changes in the $AP_{duration}$ (**Figure 4.10**), AP_{RT} (**Figure 4.11**), or AP_{FT} (**Figure 4.12**) in response in physiological pH and low pH.
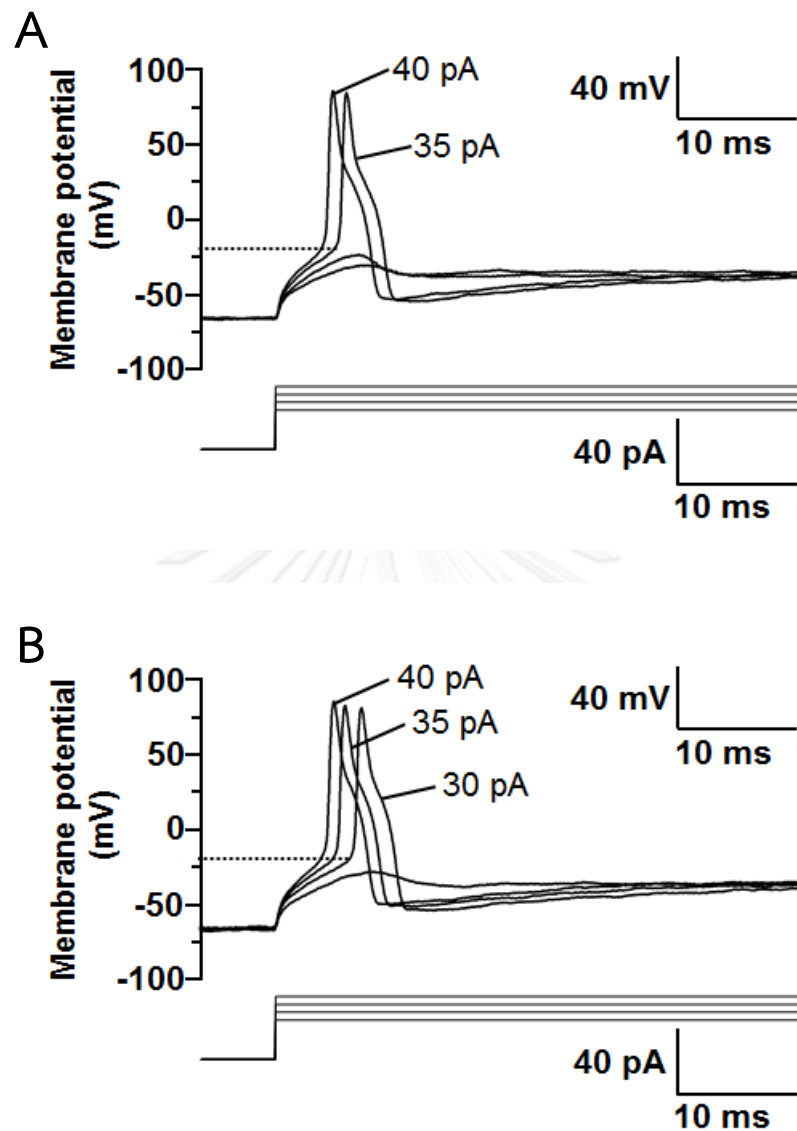
Figure 4.1 Representative traces of the excitability of small-to-medium-sized neurons that responded to physiological pH (7.4) and pH 7.0. **A.** Response of a small-to-medium-sized neuron to physiological pH showing a threshold of -21.63 mV and a rheobase of 35 pA in the first spike. **B.** Response of a small-to-medium-sized neuron to pH 7.0 showing a threshold of -23.01 mV and a rheobase of 30 pA.
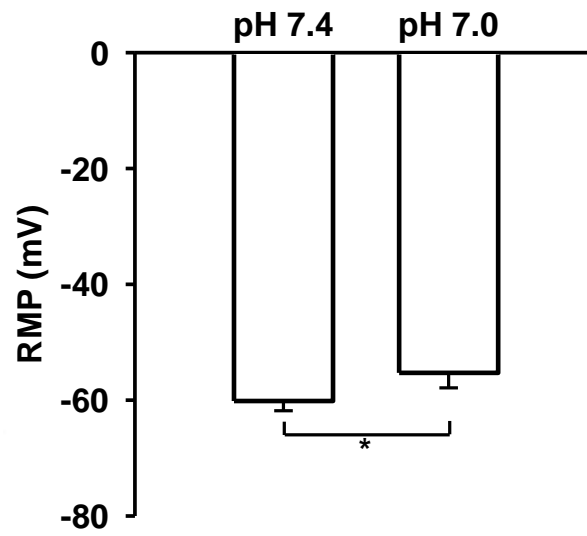
Figure 4.2 Resting membrane potential of small-to-medium-sized neurons in physiological pH (pH 7.4) compared to low pH (pH 7.0). *$P < 0.05$.
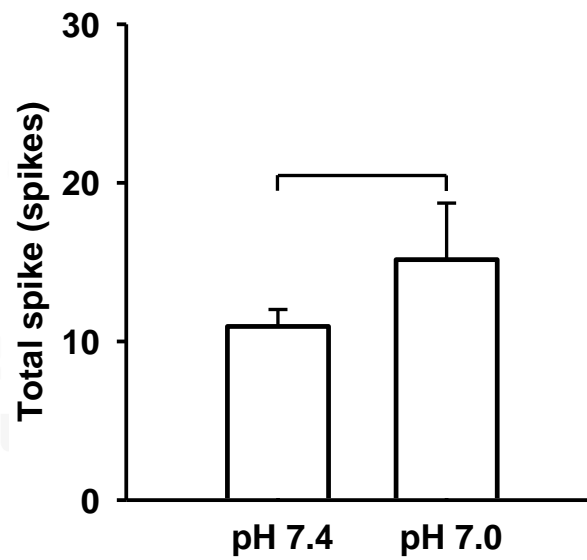
Figure 4.3 The total spike of small-to-medium-sized neurons in physiological pH (pH 7.4) compared to low pH (pH 7.0).
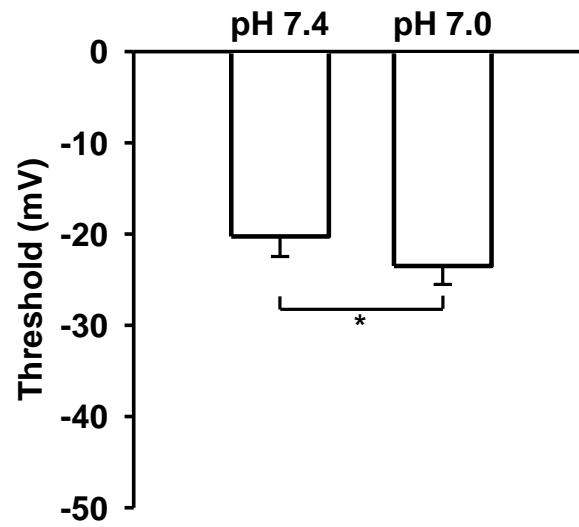
Figure 4.4 The threshold of small-to-medium-sized neurons in physiological pH (pH 7.4) compared to low pH (pH 7.0). *P < 0.05.
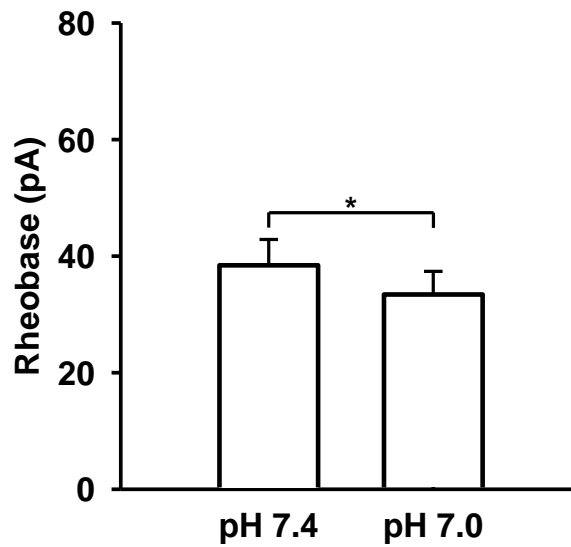
Figure 4.5 The rheobase of small-to medium-sized neurons in physiological pH (pH 7.4) compared to low pH (pH 7.0). *P < 0.05.
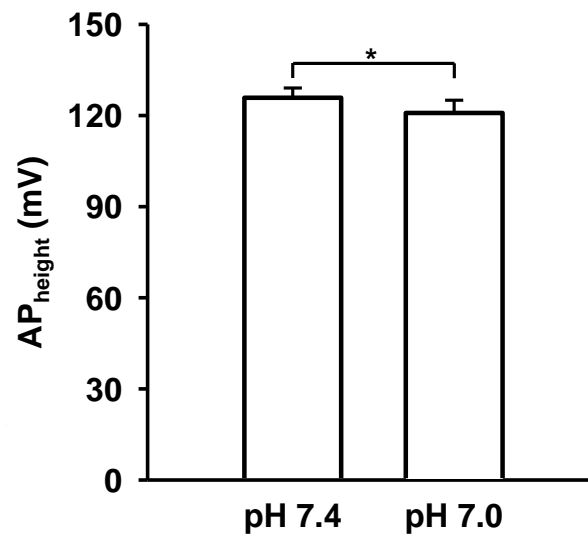
Figure 4.6 The height of action potential in small-to-medium-sized neurons in physiological pH (pH 7.4) compared to low pH (pH 7.0). *$P < 0.05$.
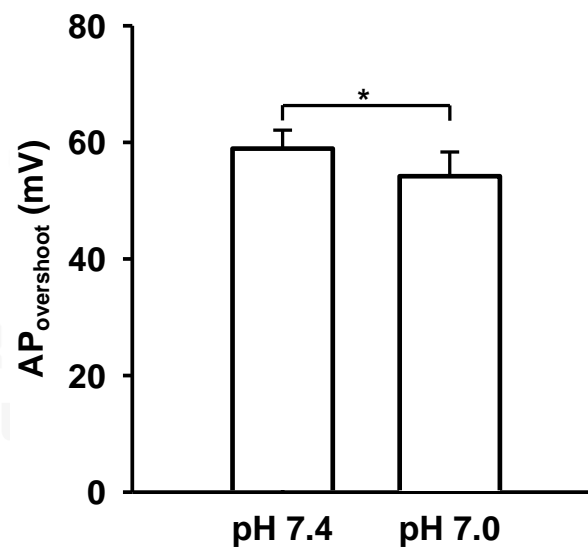
Figure 4.7 The overshoot of action potential in small-to-medium-sized neurons in physiological pH (pH 7.4) compared to low pH (pH 7.0). *$P < 0.05$.
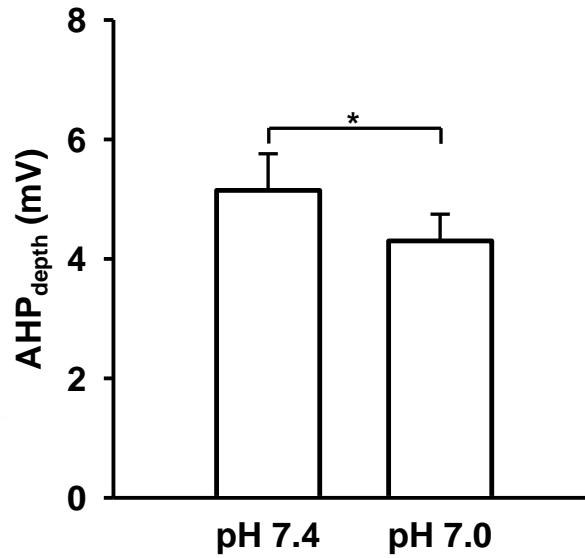
Figure 4.8 The depth of after-hyperpolarization in small-to-medium-sized neurons in physiological pH (pH 7.4) compared to low pH (pH 7.0). *$P < 0.05$.
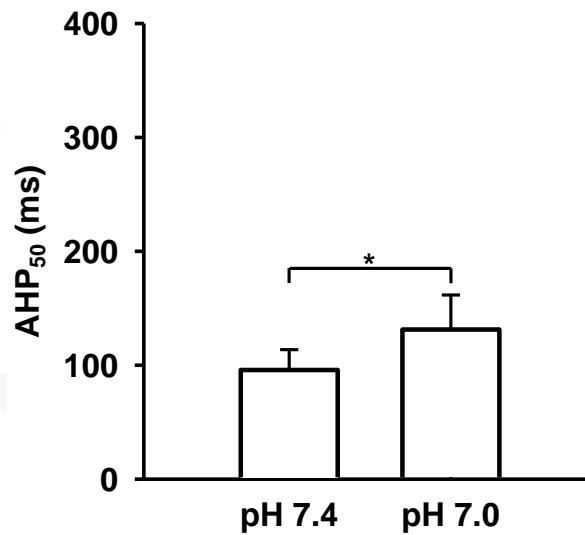
Figure 4.9 The peak of AHP to 50% recovery to baseline of after-hyperpolarization in small-to-medium-sized neurons in physiological pH (pH 7.4) compared to low pH (pH 7.0). *$P < 0.05$.
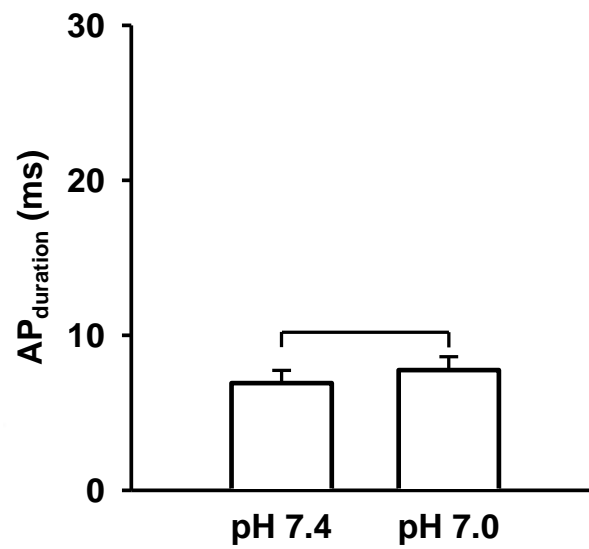
Figure 4.10 The duration of action potential in small-to medium-sized neurons in physiological pH (pH 7.4) compared to low pH (pH 7.0).
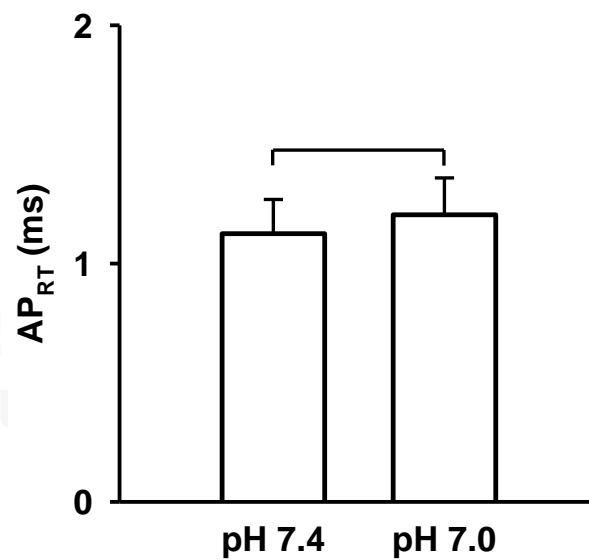
Figure 4.11 The rising time of action potential in small-to medium-sized neurons in physiological pH (pH 7.4) compared to low pH (pH 7.0).

Figure 4.12 The falling time of action potential in small-to medium-sized neurons in physiological pH (pH 7.4) compared to low pH (pH 7.0).

Table 4.1 Effect of pH change from pH 7.4 to pH 7.0 on AP variables of the small-to-medium-sized neurons

| Variables	Small–medium sized neurons (n = 19)		
	pH 7.4	pH 7.0	*P*-value
RMP (mV)	-60.15 ± 1.67	-55.28 ± 2.60*	0.010
Spike (spikes)	10.95 ± 1.07	15.16 ± 3.56	0.176
Threshold (mV)	-20.26 ± 2.20	-23.50 ± 2.02*	0.009
Rheobase (pA)	38.42 ± 4.43	33.42 ± 3.96*	0.0001
AP_{height} (mV)	125.82 ± 3.23	120.84 ± 4.20*	0.033
$AP_{overshoot}$ (mV)	58.91 ± 3.18	54.19 ± 4.16*	0.046
$AP_{duration}$ (ms)	6.91 ± 0.82	7.75 ± 0.87	0.076
AP_{RT} (ms)	1.13 ± 0.14	1.20 ± 0.15	0.412
AP_{FT} (ms)	5.79 ± 0.77	6.55 ± 0.80	0.096
AHP_{depth} (mV)	5.15 ± 0.61	4.30 ± 0.45*	0.014
AHP_{50} (ms)	95.80 ± 17.84	131.34 ± 30.33*	0.043

Neuronal properties of small-to-medium-sized neurons in physiological pH (pH 7.4) compared to low pH (pH 7.0). *$P < 0.05$. Each variable shown as mean ± SEM.

Effect of pH 7.0 on the large-sized TG neurons

Depolarizing current pulses with 500 ms were applied to the large-sized neurons (>40 μm, *n* = 6) before and after decreasing the pH from physiological (pH 7.4) to low pH (pH 7.0) as shown in representative traces (**Figure 4.13**). The RMP was not significantly different between physiological pH and pH 7.0 (**Figure 4.14** and **Table 4.2**). Responding neurons were not significantly excitable at pH 7.0 (**Table 4.2**). There was no significant difference between the numbers of spikes during pH change (**Figure 4.15**). Moreover, the threshold was not changed at pH7.0 (**Figure 4.16**), and the rheobase was also unchanged at pH 7.0 (**Figure 4.17**).

There were no significant differences in the variables of AP shape (**Table 4.2**). The AP_{height} was not changed at pH7.0 (**Figure 4.18**) and the $AP_{overshoot}$ was also not changed at pH 7.0 (**Figure 4.19**). Similarly, the AHP_{depth} was not changed at pH 7.0 (**Figure 4.20**) and the AHP_{50} was also not changed at pH 7.0 (**Figure 4.21**). Moreover, the $AP_{duration}$ (**Figure 4.22**), AP_{RT} (**Figure 4.23**), and AP_{FT} (**Figure 4.24**) were not significantly changed in response to pH.
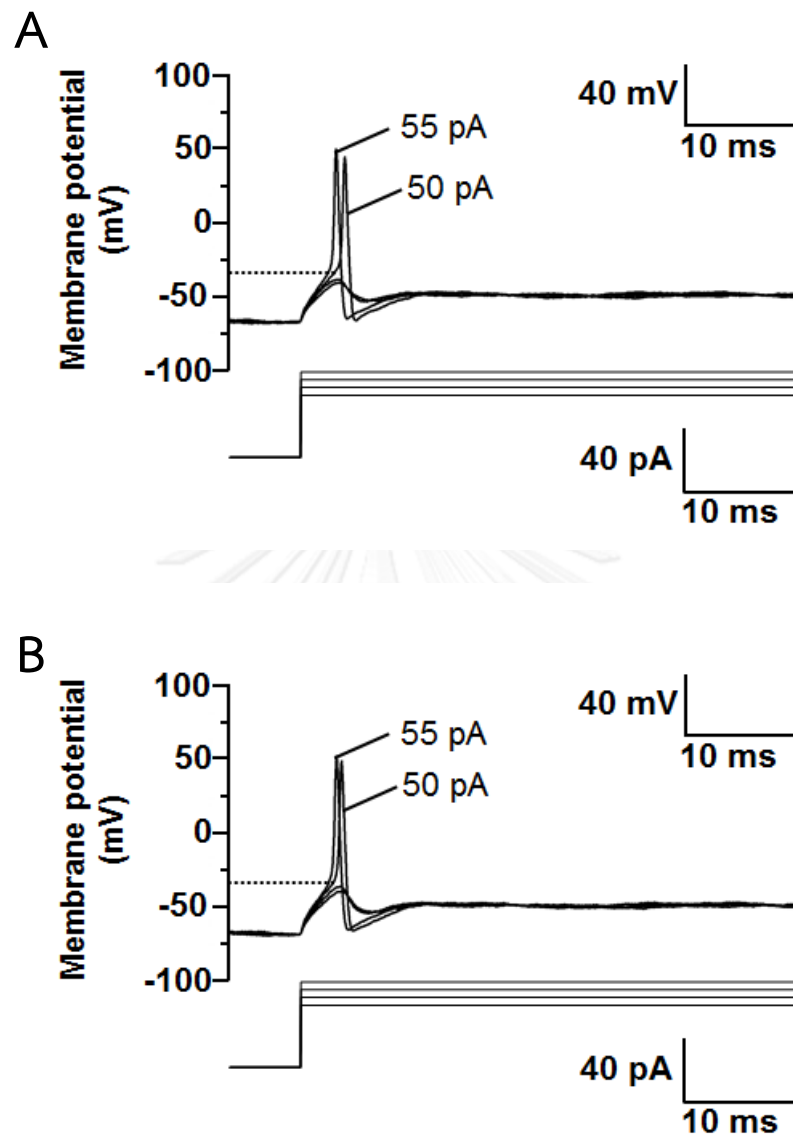
Figure 4.13 Representative traces of the excitability of large-sized neurons that responded to physiological pH (7.4) and low pH (pH7.0). **A.** Response of a large-sized neuron to physiological pH showing a threshold of -33.48 mV and a rheobase of 50 pA. **B.** Response of a large-sized neuron to pH 7.0 showing a threshold of -33.42 mV and a rheobase of 50 pA.
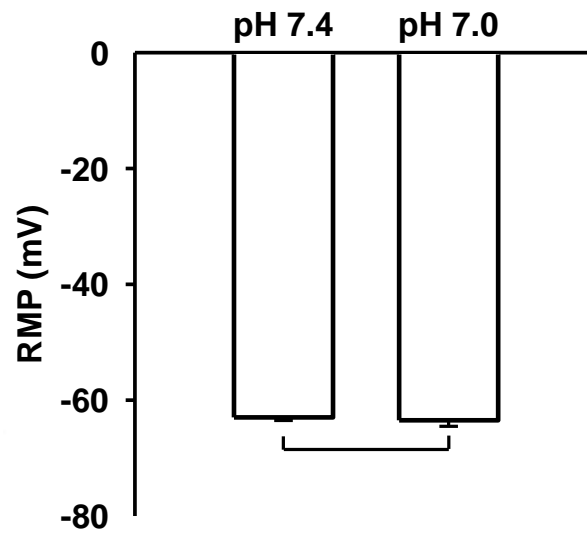
Figure 4.14 The resting membrane potential of large-sized neurons in physiological pH (pH 7.4) compared to low pH (pH 7.0).
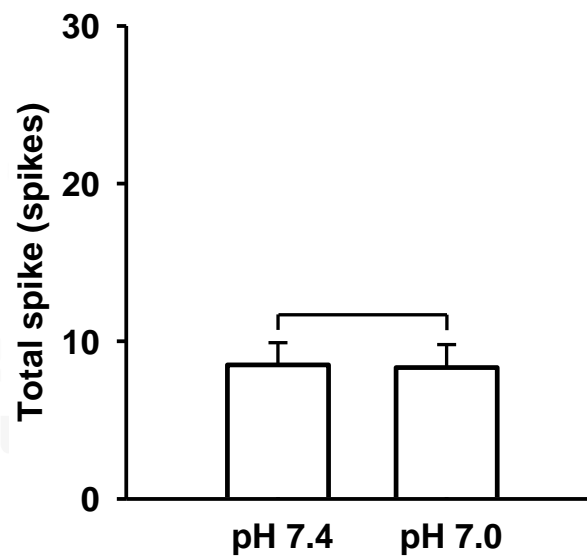
Figure 4.15 The total spike large-sized neurons in physiological pH (pH 7.4) compared to low pH (pH 7.0).
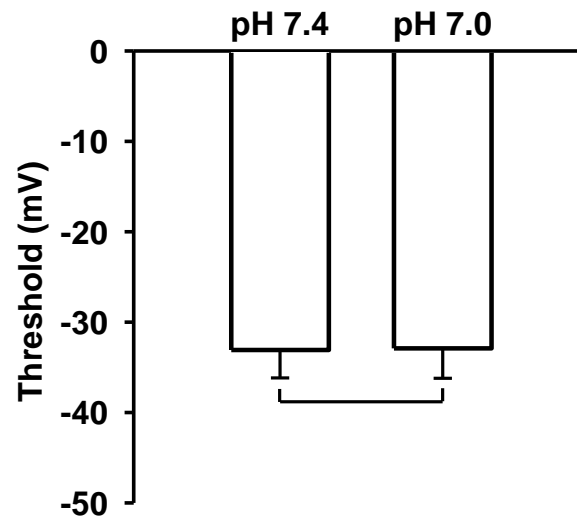
Figure 4.16 Threshold of large-sized neurons in physiological pH (pH 7.4) compared to low pH (pH 7.0).
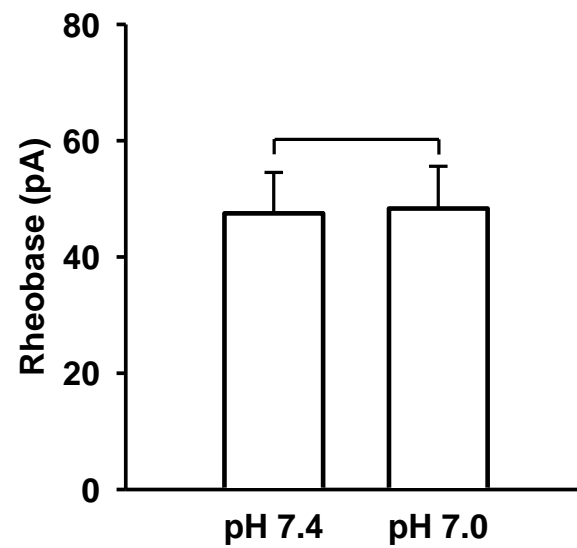
Figure 4.17 The rheobase of large-sized neurons in physiological pH (pH 7.4) compared to low pH (pH 7.0).
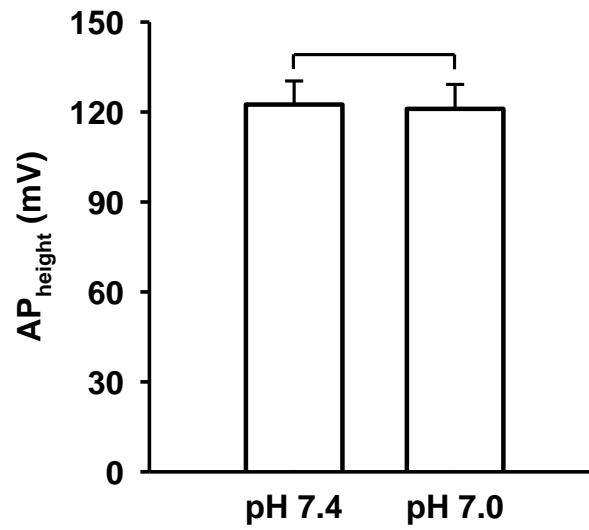
Figure 4.18 The height of action potential in large-sized neurons in physiological pH (pH 7.4) compared to low pH (pH 7.0).

**Figure 4.19** The overshoot of action potential in large-sized neurons in physiological pH (pH 7.4) compared to low pH (pH 7.0).

Figure 4.20 The depth of after-hyperpolarization in large-sized neurons in physiological pH (pH 7.4) compared to low pH (pH 7.0).

Figure 4.21 The peak of AHP to 50% recovery to baseline of after-hyperpolarization in large-sized neurons in physiological pH (pH 7.4) compared to low pH (pH 7.0).

Figure 4.22 The duration of action potential in large-sized neurons in physiological pH (pH 7.4) compared to low pH (pH 7.0).

Figure 4.23 The rising time of action potential in large-sized neurons in physiological pH (pH 7.4) compared to low pH (pH 7.0).
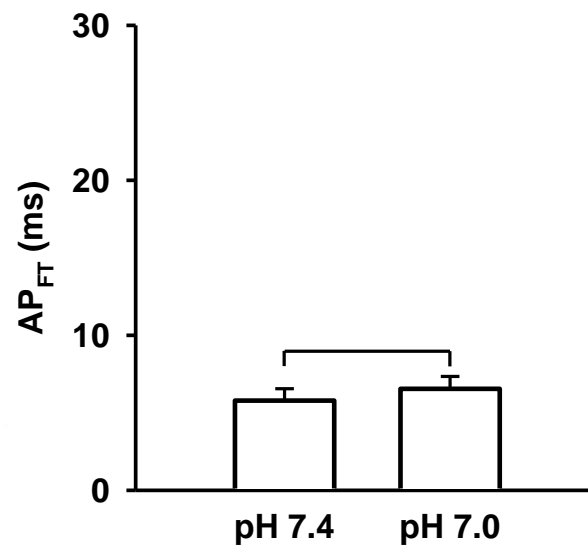
Figure 4.24 The falling time of action potential in large-sized neurons in physiological pH (pH 7.4) compared to low pH (pH 7.0).

Table 4.2 Effect of pH 7.0 on AP variables of the large-sized neurons

Variables	Large-sized neurons (n = 6)		
	pH 7.4	pH 7.0	*P*-value
RMP (mV)	-61.98 ± 0.52	-63.48 ± 1.03	0.577
Spike (spikes)	8.50 ± 1.41	8.33 ± 1.45	0.741
Threshold (mV)	-33.08 ± 3.09	-32.90 ± 3.32	0.828
Rheobase (pA)	47.50 ± 7.04	48.33 ± 7.26	0.741
AP_{height} (mV)	122.47 ± 7.87	121.03 ± 8.17	0.477
$AP_{overshoot}$ (mV)	55.83 ± 8.06	53.90 ± 8.21	0.305
$AP_{duration}$ (ms)	13.29 ± 10.05	11.91 ± 8.04	0.530
AP_{RT} (ms)	1.20 ± 0.27	1.34 ± 0.21	0.493
AP_{FT} (ms)	12.09 ± 10.00	10.58 ± 7.98	0.491
AHP_{depth} (mV)	5.47 ± 0.81	5.02 ± 0.78	0.101
AHP_{50} (ms)	153.62 ± 47.65	227.58 ± 80.07	0.105

Neuronal properties of large-sized neuron in physiological pH (pH 7.4) compared to low pH (pH 7.0). Each variable is shown as mean ± SEM.

Effect of CGRP in modulating pH 7.0 on the small-to-medium-sized neurons

Depolarizing current pulses with 500 ms were applied to the small-to-medium-sized neurons (<40 μm, *n* = 9) treated with CGRP before and after decreasing the pH from physiological (pH 7.4) to pH 7.0 as shown in representative trace (**Figure 4.25).** The RMP was significantly shifted to more negative when pH was decreased from physiological pH to pH 7.0 (**Figure 4.26** and **Table 4.3**). There was no significant difference between the numbers of spikes before and after decreasing the pH (**Figure 4.27**). The threshold at physiological pH was shifted to less negative at pH 7.0 (**Figure 4.28**), while the rheobase of current at physiological pH was decreased at pH 7.0 (**Figure 4.29**), but this was not significantly different (**Table 4.3**).

The AP_{height} at physiological pH was significantly reduced when pH was change to pH 7.0 (**Figure 4.30**) and the $AP_{overshoot}$ was significantly reduced (**Figure 4.31**). The AHP_{depth} was significantly increased (**Figure 4.32**), while the AHP_{50} showed no difference between physiological pH and pH 7.0 (**Figure 4.33**). There were no significant difference in the $AP_{duration}$ (**Figure 4.34)** and AP_{FT} (**Figure 4.35**). By contrast, the AP_{RT} at physiological pH was significantly longer at pH7.0 ((**Figure 4.36** and **Table 4.3**).

Figure 4.25 Representative traces present the neuronal excitability of small-to-medium-sized neurons that responded to physiological pH (7.4) and low pH (pH 7.0) with CGRP application. **A.** Response of a small-to-medium-sized neuron to pH 7.4 showing a threshold of -27.59 mV and a rheobase of 30 pA in the first spike. **B.** Response of a small-to-medium-sized neuron to pH 7.0 showing a threshold of -28.11 mV and a rheobase of 30 pA.

Figure 4.26 The resting membrane potential of small-to medium-sized neurons in physiological pH (pH 7.4) compared to low pH (pH 7.0) with CGRP application. *$P <$ 0.05.

Figure 4.27 The total spike of small-to-medium-sized neurons in physiological pH (pH 7.4) compared to low pH (pH 7.0) with CGRP application.

Figure 4.28 The threshold of small-to-medium-sized neurons in physiological pH (pH 7.4) compared to low pH (pH 7.0) with CGRP application.

Figure 4.29 The rheobase of small-to-medium-sized neurons in physiological pH (pH 7.4) compared to low pH (pH 7.0) with CGRP application.

Figure 4.30 The height of action potential in small-to-medium-sized neurons in physiological pH (pH 7.4) compared to low pH (pH 7.0) with CGRP application. *$P <$ 0.05.
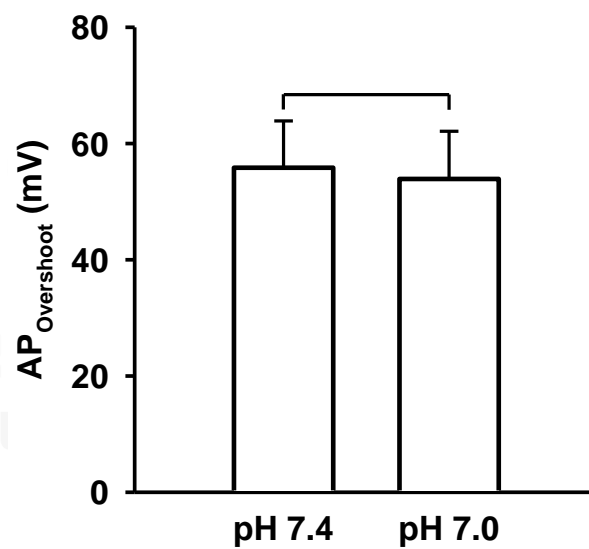

Figure 4.31 The overshoot of action potential in small-to-medium-sized neurons in physiological pH (pH 7.4) compared to low pH (pH 7.0) with CGRP application. *$P <$ 0.05.
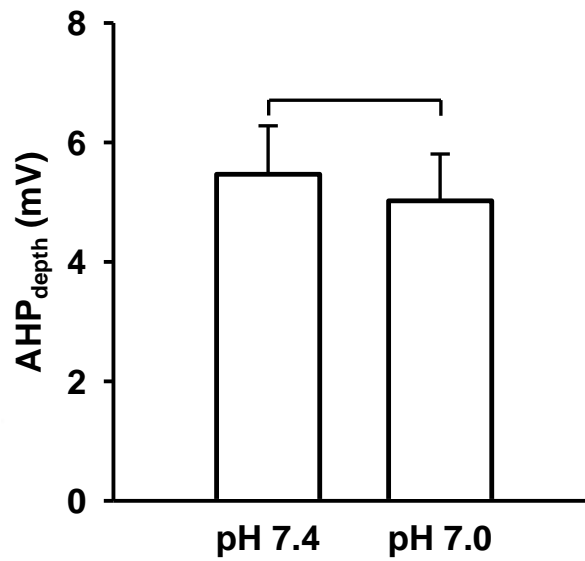
Figure 4.32 The depth of after-hyperpolarization in small-to-medium-sized neurons in physiological pH (pH 7.4) compared to low pH (pH 7.0) with CGRP application. *$P <$ 0.05.
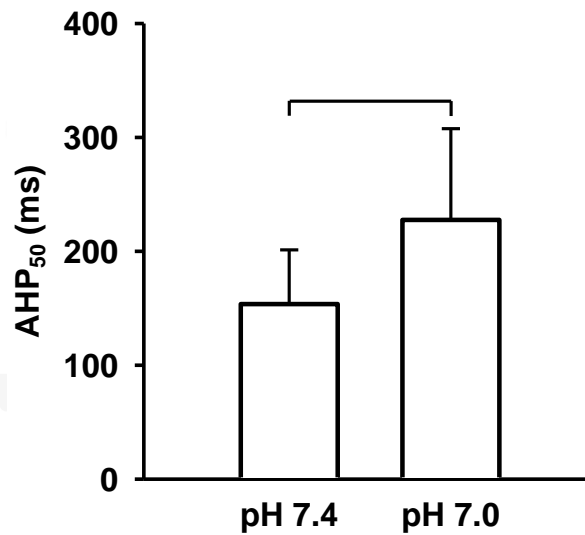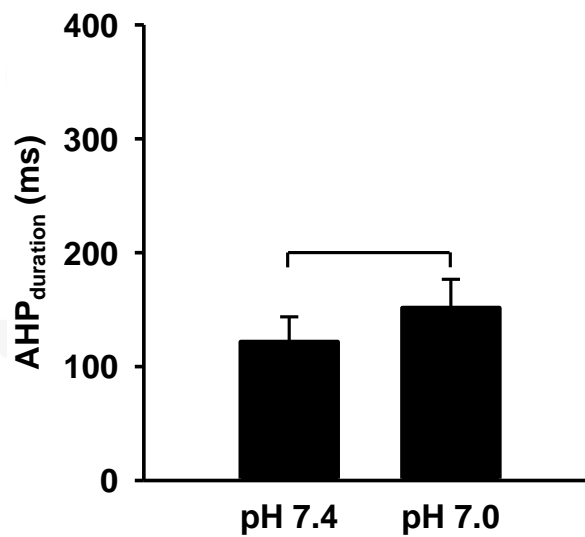

Figure 4.33 The peak of AHP to 50% recovery to baseline of afterhyperpolarization in small-to-medium-sized neurons in physiological pH (pH 7.4) compared to low pH (pH 7.0) with CGRP application.
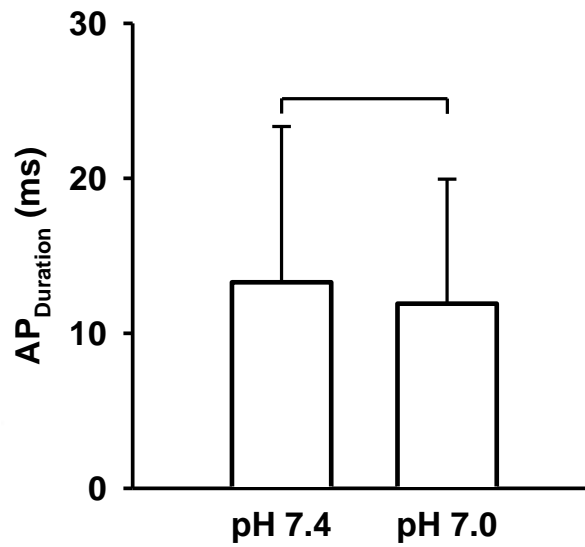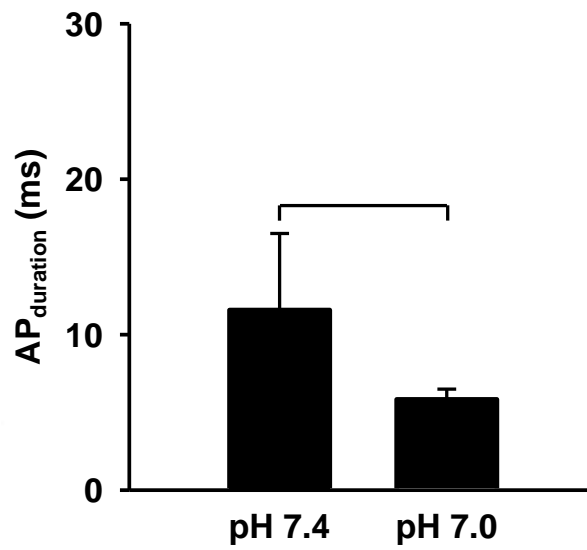
Figure 4.34 The duration of action potential in small-to-medium-sized neurons in physiological pH (pH 7.4) compared to low pH (pH 7.0) with CGRP application.
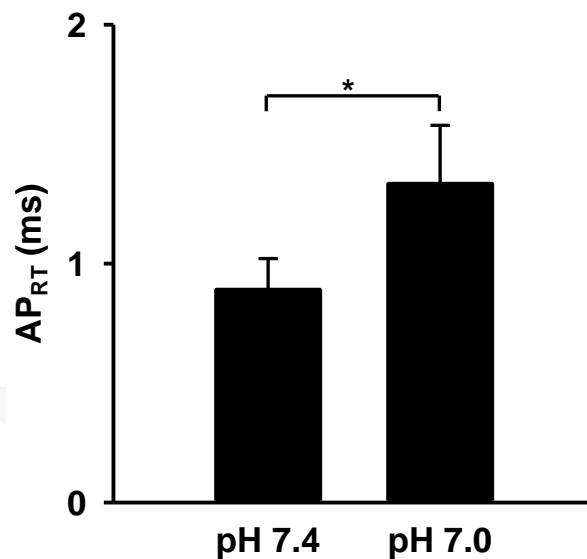
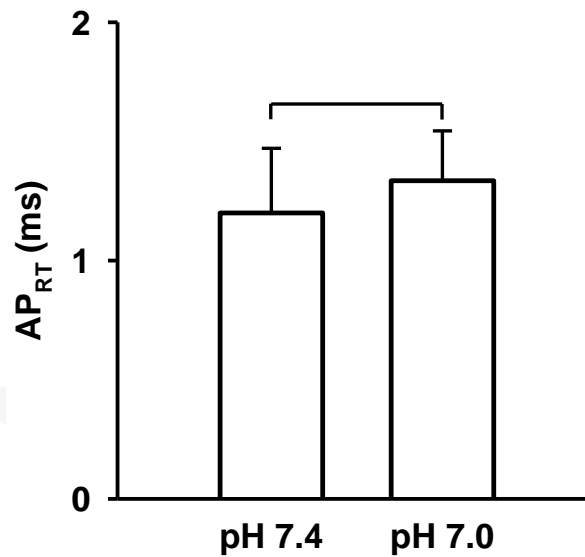**Figure 4.35** The rising time of action potential in small-to-medium-sized neurons in physiological pH (pH 7.4) compared to low pH (pH 7.0) with CGRP application. *$P <$ 0.05.
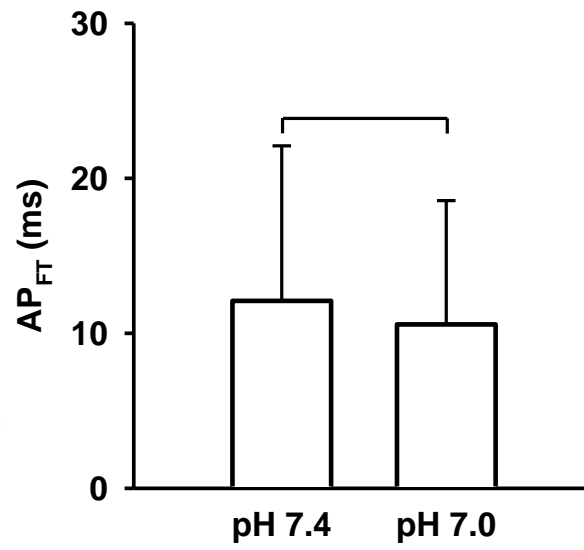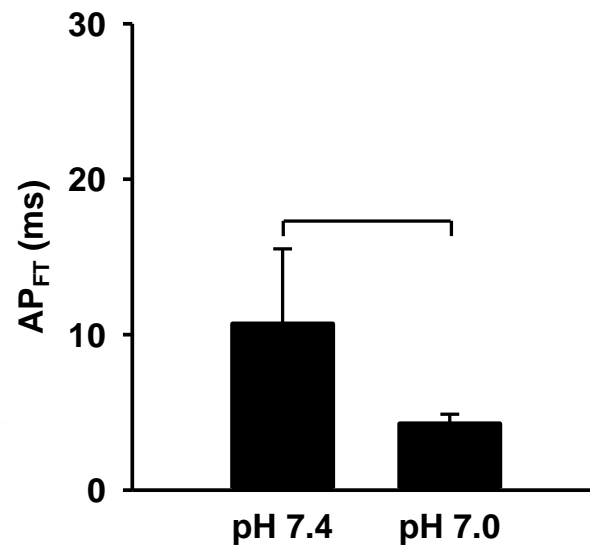
Figure 4.36 The falling time of action potential in small-to medium-sized neurons in physiological pH (pH 7.4) compared to low pH (pH 7.0) with CGRP application.

Table 4.3 Effect of pH 7.0 with CGRP on AP variables of the small–medium sized neurons

Variables	Small–medium sized neurons (n = 9)		
	pH 7.4	pH 7.0	*P*-value
RMP (mV)	-59.14 ± 2.00	-64.71 ± 3.19*	0.015
Spike (spikes)	10.11 ± 1.95	8.89 ± 2.30	0.111
Threshold (mV)	-25.41 ± 1.99	-17.95 ± 4.05	0.080
Rheobase (pA)	39.44 ± 9.73	25.56 ± 9.22	0.212
AP_{height} (mV)	133.88 ± 3.06	123.44 ± 5.82*	0.014
$AP_{overshoot}$ (mV)	67.23 ± 2.99	55.88 ± 5.88*	0.011
$AP_{duration}$ (ms)	11.58 ± 4.92	5.83 ± 0.66	0.276
AP_{RT} (ms)	0.89 ± 0.13	1.33 ± 0.25*	0.013
AP_{FT} (ms)	10.70 ± 4.82	4.27 ± 0.61	0.226
AHP_{depth} (mV)	4.02 ± 0.88	5.85 ± 0.70*	0.003
AHP_{50} (ms)	127.55 ± 22.08	151.36 ± 25.23	0.123

Neuronal properties of small-to-medium-sized neurons in physiological pH (pH 7.4) compared to low pH (pH 7.0) with CGRP application. *$P < 0.05$. Each variable is shown as mean ± SEM.

Effect of CGRP in modulating pH 7.0 on the large-sized neurons

Depolarizing current pulses with 500 ms were applied to the large-sized neurons (>40 μm, *n* = 6) that were applied with CGRP in physiological pH (pH 7.4) compared to low pH (pH 7.0) (**Figure 4.37).** The RMP was not changed at pH 7.0 (**Figure 4.38** and **Table 4.4**). Large-sized neurons in pH 7.4 showed significantly less spikes at than at pH7.0 (**Figure 4.39**). The threshold was not significantly changed (**Figure 4.40**), but the rheobase of current at pH 7.4 was significantly decreased comparing with at pH 7.0 (**Figure 4.41** and **Table 4.4**).

The AP_{height} at physiological pH was not significantly changed at pH 7.0 (**Figure 4.42**) and the $AP_{overshoot}$ was also not significantly changed at pH 7.0 (**Figure 4.43**). The AHP_{depth} was not significantly changed at pH 7.0 (**Figure 4.44**) and the AHP_{50} was also not changed at pH 7.0 (**Figure 4.45**). Moreover, the $AP_{duration}$ (**Figure 4.46),** AP_{RT} (**Figure 4.47),** and AP_{FT} (**Figure 4.48)** were not significantly changed in response to pH 7.0 (**Table 4.4**).
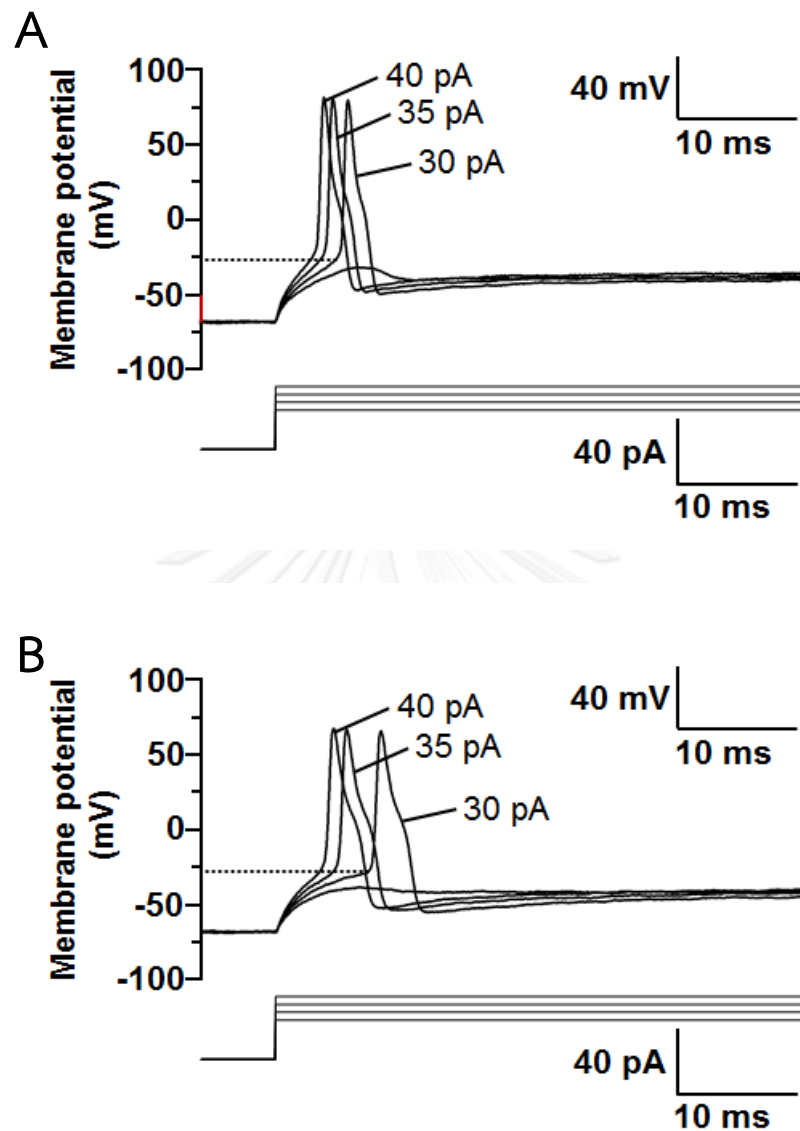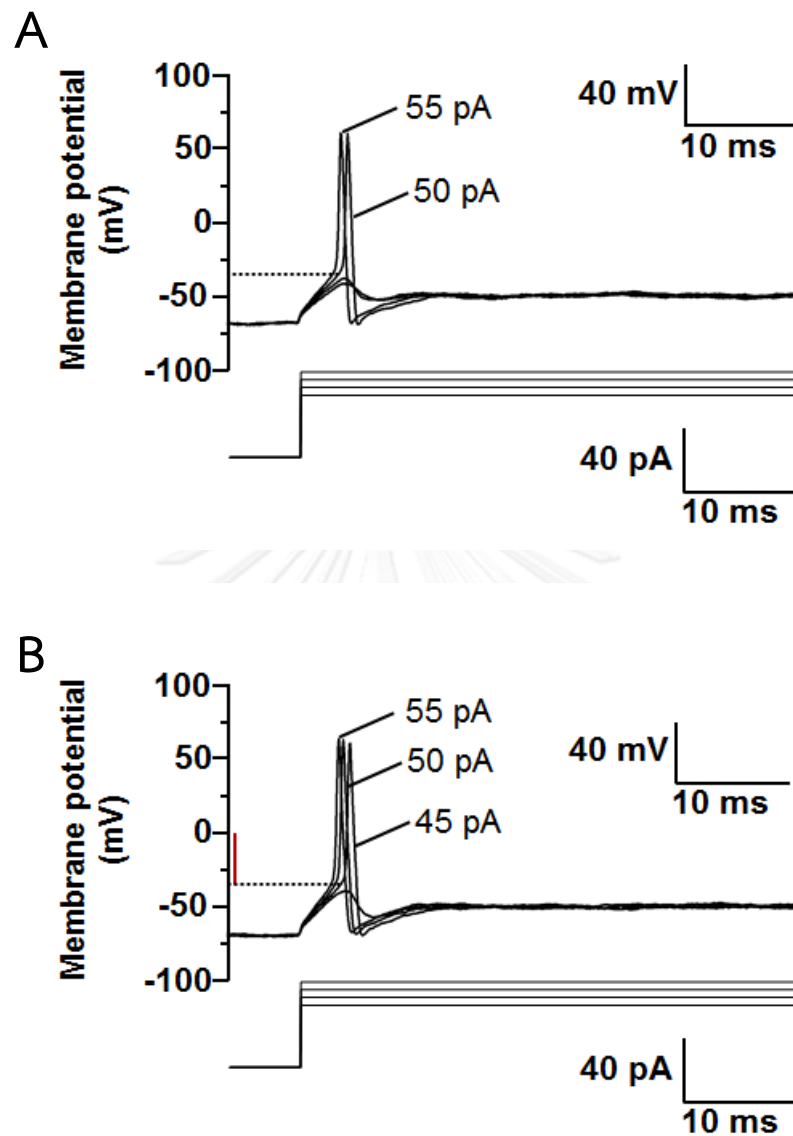
Figure 4.37 Representative traces show the neuronal excitability of large-sized neurons that responded to physiological pH (7.4) and low pH (pH 7.0) with CGRP application. **A.** Response of a large-sized neuron to pH 7.4 showing a threshold of -34.74 mV and a rheobase of 50 pA. **B.** Response of a large-sized neuron to pH 7.0 showing a threshold of -34.43 mV and a rheobase of 45 pA.
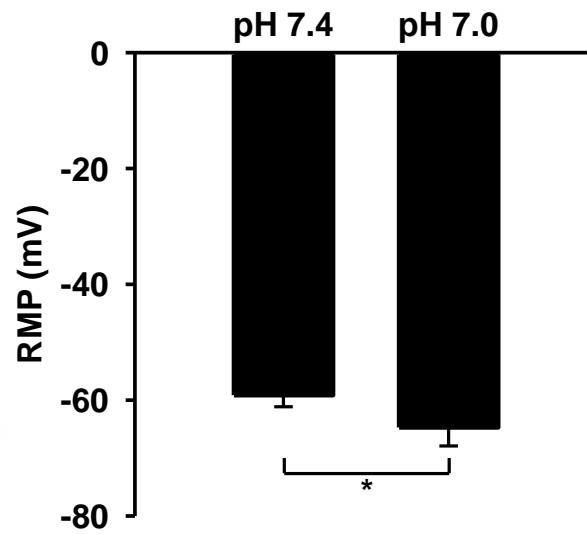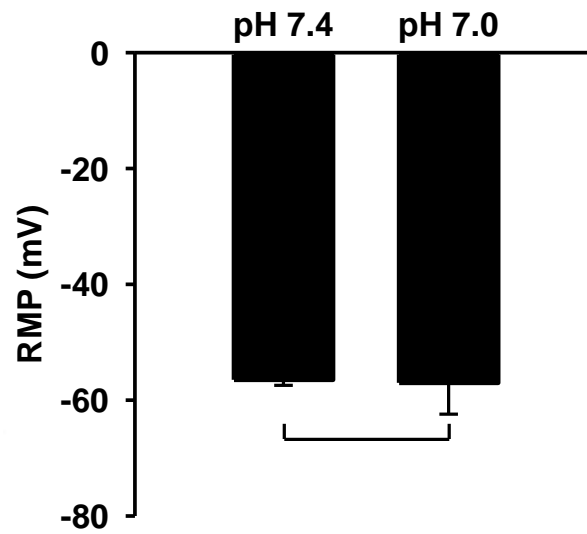
Figure 4.38 The resting membrane potential of large-sized neurons in physiological pH (pH 7.4) compared to low pH (pH 7.0) with CGRP application.
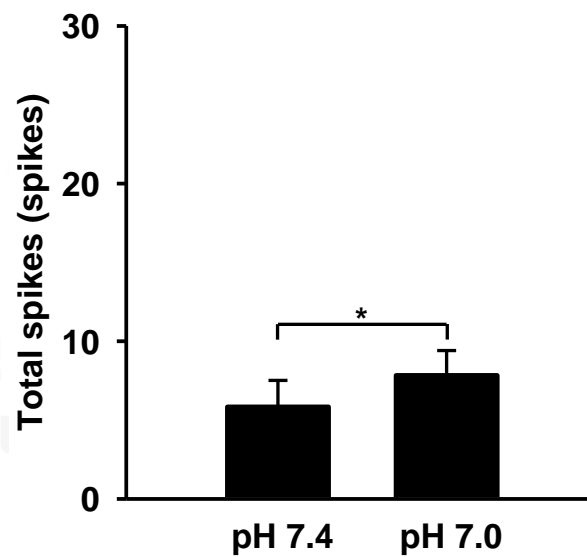
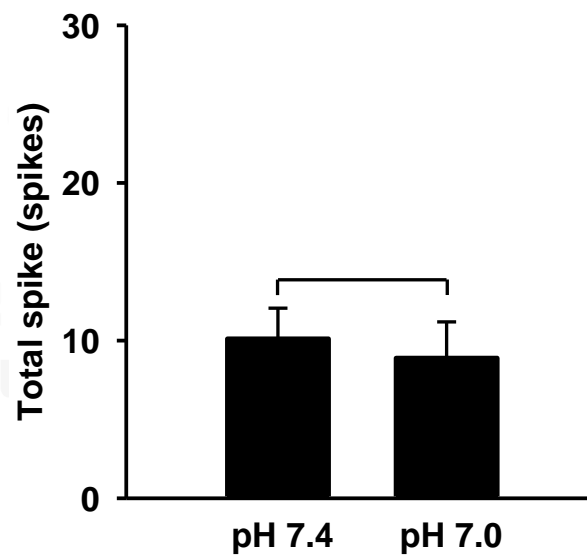**Figure 4.39** The total spike of large-sized neurons in physiological pH (pH 7.4) compared to low pH (pH 7.0) with CGRP application. *$P < 0.05$.
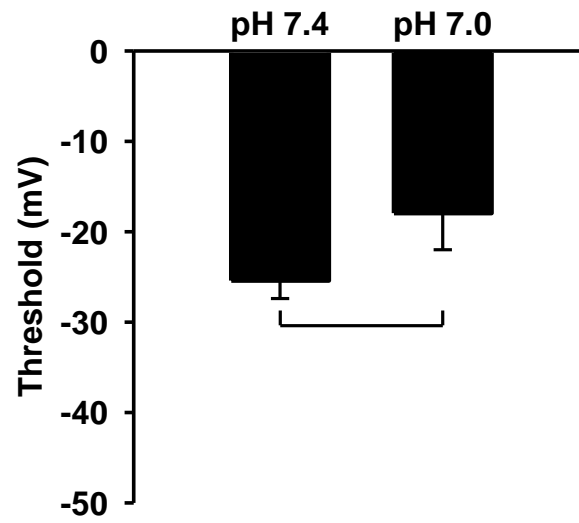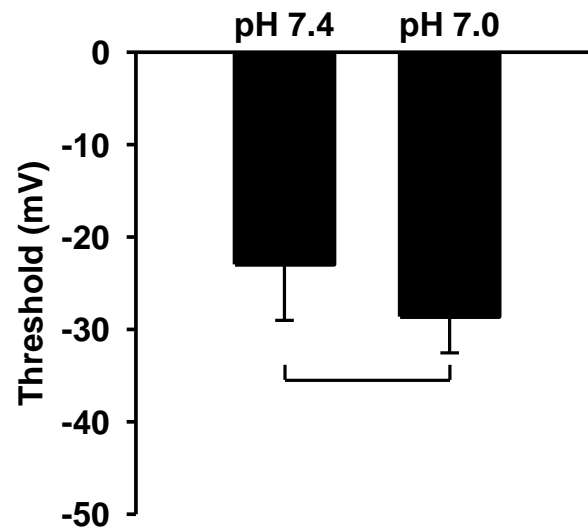
Figure 4.40 The threshold of large-sized neurons in physiological pH (pH 7.4) compared to low pH (pH 7.0) with CGRP application.
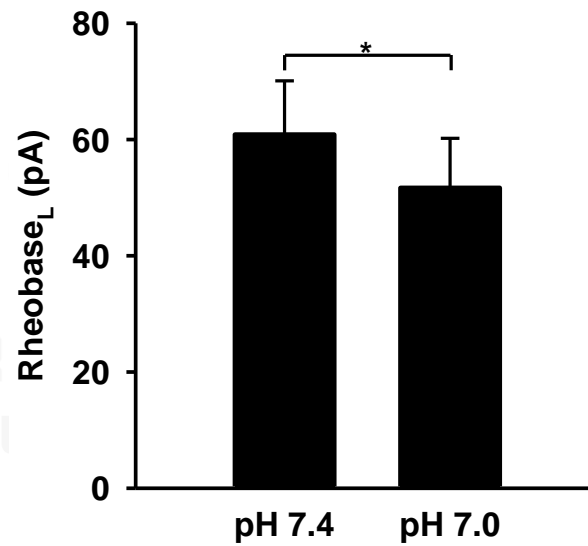
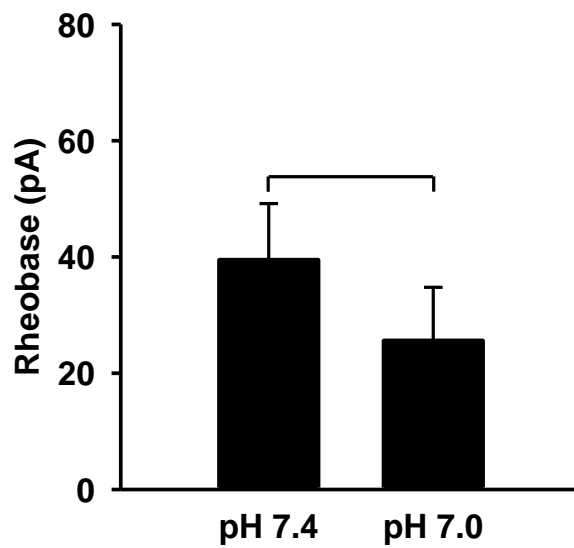**Figure 4.41** The rheobase of large-sized neurons in physiological pH (pH 7.4) compared to low pH (pH 7.0) with CGRP application. *$P < 0.05$.
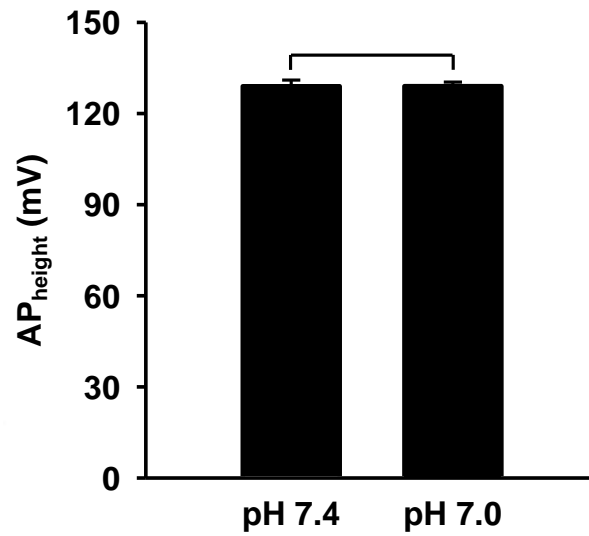
Figure 4.42 The height of action potential in large-sized neurons in physiological pH (pH 7.4) compared to low pH (pH 7.0) with CGRP application.
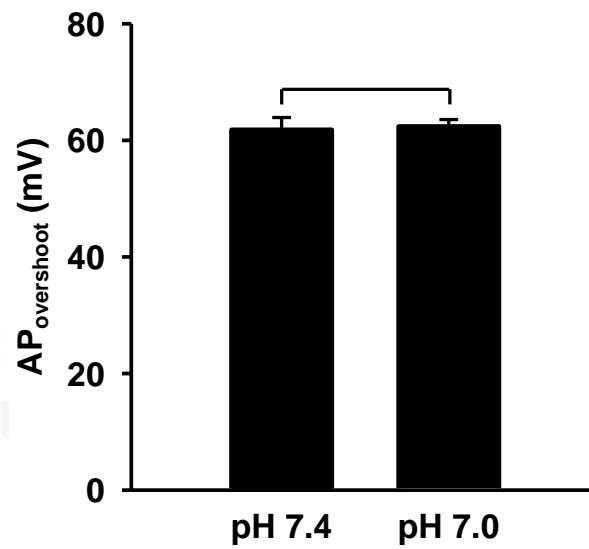
Figure 4.43 The overshoot of action potential in large-sized neurons in physiological pH (pH 7.4) compared to low pH (pH 7.0) with CGRP application.
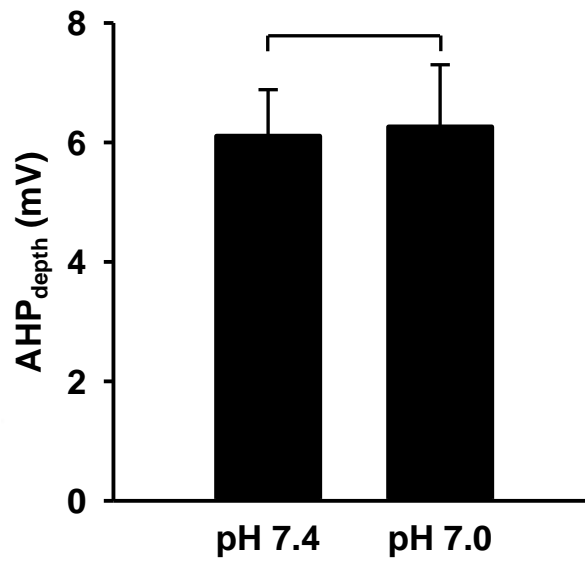
Figure 4.44 The depth of after-hyperpolarization in large-sized neurons in physiological pH (pH 7.4) compared to low pH (pH 7.0) with CGRP application.
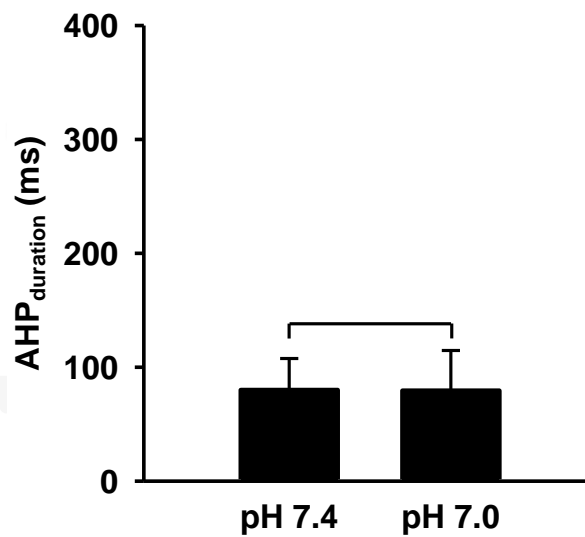
Figure 4.45 The peak of AHP to 50% recovery to baseline of after-hyperpolarization in large-sized neurons in physiological pH (pH 7.4) compared to low pH (pH 7.0) with CGRP application.
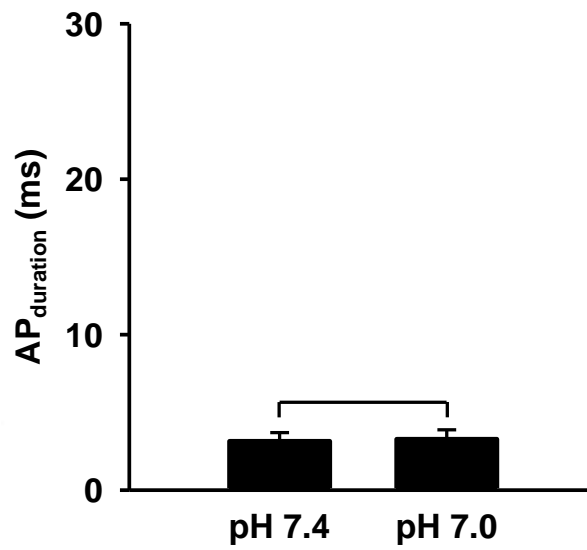
Figure 4.46 The duration of action potential in large-sized neurons in physiological pH (pH 7.4) compared to low pH (pH 7.0) with CGRP application.
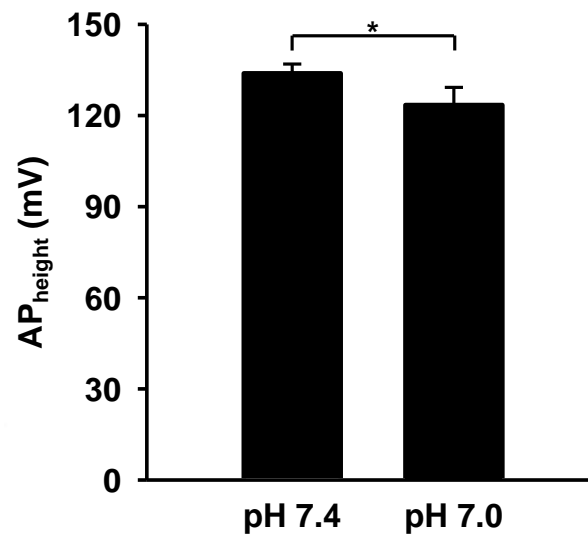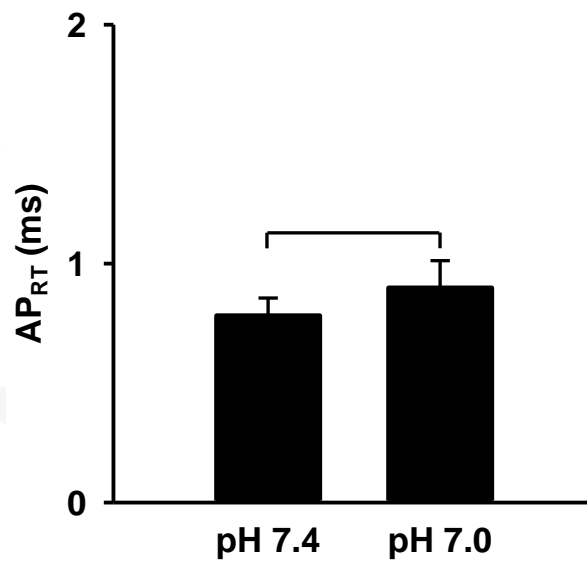

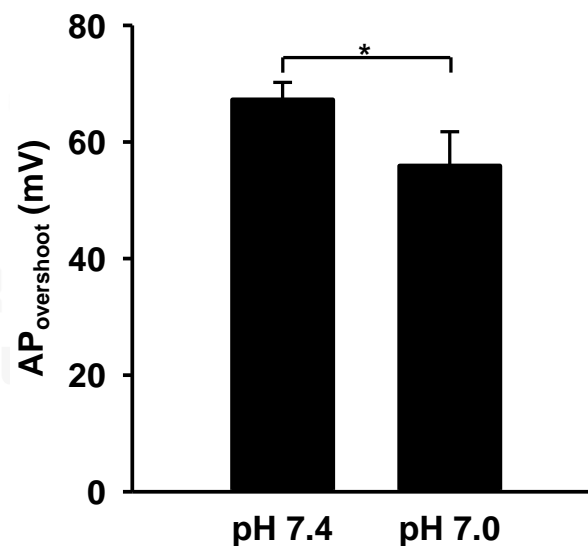**Figure 4.47** The rising time of action potential in large-sized neurons in physiological pH (pH 7.4) compared to low pH (pH 7.0) with CGRP application.
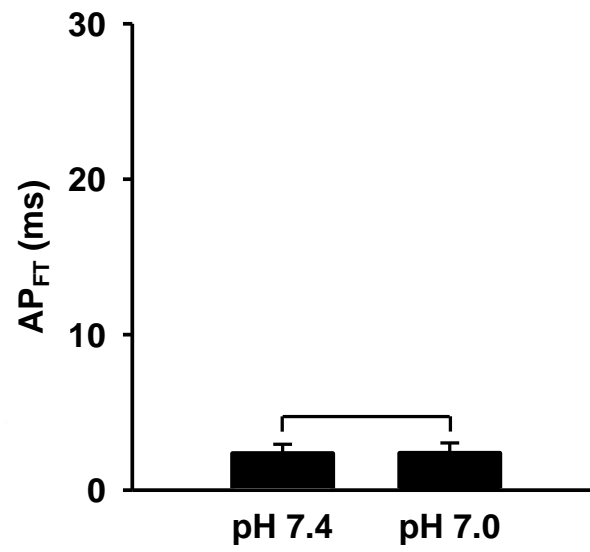
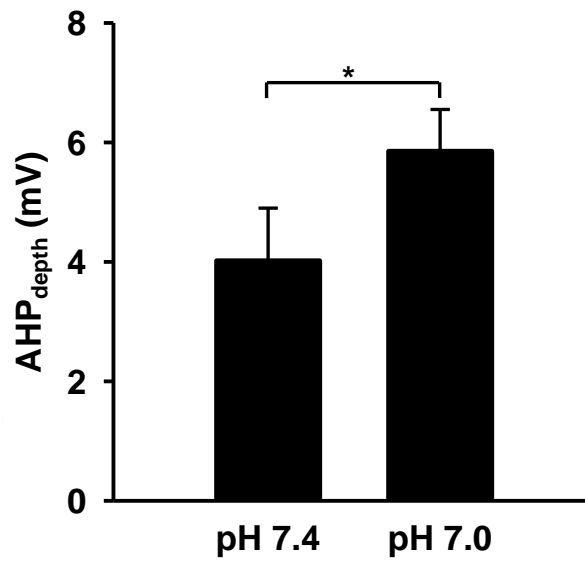**Figure 4.48** The falling time of action potential in large-sized neurons in physiological pH (pH 7.4) compared to low pH (pH 7.0) with CGRP application.

Table 4.4 Effect of pH 7.0 with CGRP on AP variables of the large-sized neurons

| Variables | Large-sized neurons (n = 6) | | |
	pH 7.4	pH 7.0	*P*-value
RMP (mV)	-56.48 ± 0.97	-57.02 ± 5.40	0.918
Spike (spikes)	5.83 ± 1.68	7.83 ± 1.58*	0.001
Threshold (mV)	-22.96 ± 6.06	-28.62 ± 3.92	0.296
Rheobase (pA)	60.83 ± 9.26	51.67 ± 8.53*	0.002
AP_{height} (mV)	128.97 ± 2.03	128.98 ± 1.35	0.990
$AP_{overshoot}$ (mV)	61.80 ± 2.11	62.38 ± 1.19	0.682
$AP_{duration}$ (ms)	3.14 ± 0.56	3.27 ± 0.60	0.753
AP_{RT} (ms)	0.78 ± 0.07	0.90 ± 0.11	0.255
AP_{FT} (ms)	2.36 ± 0.59	2.37 ± 0.66	0.970
AHP_{depth} (mV)	6.10 ± 0.78	6.26 ± 1.04	0.887
AHP_{50} (ms)	79.98 ± 27.70	79.37 ± 35.28	0.972

Neuronal properties of large-sized neurons in physiological pH (pH 7.4) compared to low pH (pH 7.0) with CGRP application. *$P < 0.05$. Each variable is shown as mean ± SEM.

CHAPTER V

DISCUSSIONS

The present study had purposed to demonstrate the effect of CGRP on ASICs in trigeminal ganglion neurons.

Effect of pH 7.0 on the small-to-medium-sized TG neurons

Extracellular proton (pH 7.0) alters an excitability of small-to-medium-sized neurons by depolarizing RMP, reducing threshold and rheobase. Moreover, extracellular proton also changes AP shapes by decreasing height and overshoot, as well as reducing the depth of AHP and lengthening the duration of AHP_{50}.

RMP is generally stabilized by two-pore potassium channel (K2P) or called 'leak-channel', voltage-gated sodium channels 1.9 ($Na_V1.9$), and voltage-gated potassium channels 7.2-7.3 ($K_V7.2$-7.3). These channels are activated at membrane potential near RMP or below, especially K2P that is activated at more negative membrane potential than the others (106-108). Our results showed that RMP was depolarized by pH 7.0. This indicated that the effect of extracellular proton inhibits subtypes of K2P, which were TWIK (two pore domain potassium channel)-related acid sensitive K^+ channel 3 (TASK-3) and TWIK-related spinal cord K^+ channel (TRESK), and then potassium (K^+) ions cannot efflux or leak out through these channels resulting in accommodation of intracellular K^+ ion (109-111). Meanwhile, extracellular proton activates ASICs resulting in the Na^+ passing into neurons (21, 85). The accommodation of intracellular Na^+ and K^+ shifts RMP value to more positive, therefore neuronal excitability is increased.

Threshold is the critical level that the inward Na^+ ion exceeds the outward K^+ and Cl^- ions. This depolarization causes the activation of voltage-gated sodium channels (Na_V) and AP induction. Incidentally, rheobase (threshold current) is the value of injected current that shift membrane potential to threshold. The subtypes of Na_V channels which regulated depolarization toward threshold are $Na_V1.7$ and 1.9 channels (112, 113). These channels are activated under the threshold (or called

'subthreshold'), and they shift membrane potential closing to threshold for opening $Na_V1.8$ that produces upstroke of AP (112). Our results showed that threshold was decreased to more negative and rheobase was reduced in the condition of pH 7.0. These may cause from an up-regulation of $Na_V1.9$, which may be regulated via ASICs signaling pathway. This indication is similarly to effect of PGE_2 that up-regulated $Na_V1.9$ via G-proteins signaling (114, 115). Moreover, threshold decreasing and rheobase reduction may be the result of an internal dialysis of GTP that modulates and up-regulates $Na_V1.9$ (116). Interestingly, we used GTP in an intracellular solution (see the methods) and shifted the pH from 7.4 to 7.0 approximately 10 minutes that GTP would be internally dialyzed. Indeed, the effect the internal dialysis of GTP on threshold and rheobase has been investigating (117). In addition to $Na_V1.9$, the up-regulation of $Na_V1.7$ under inflammatory condition can reduce rheobase and amplifying sub-threshold depolarization to reach the threshold of $Na_V1.8$ for producing AP (112). Thus, under the condition of pH 7.0, threshold and rheobase are modulated by $Na_V1.7$ and $Na_V1.9$, which both channels are possibly up-regulated via G-protein signaling pathway of ASICs. These cause the neuronal excitability that will reach the threshold for triggering AP.

AP is driven by Na^+ influx that passes through NaV1.7 and $Na_V1.8$ during the depolarization state. The pore of voltage-gated sodium channels (Na_V) consists of four domains (DI-DIV), which each domain comprises from six trans-membrane segments (S1-S6) (118). While S1-S4 segments functions as the voltage sensing domain (VSD), S5-S6 segments forms the pore module (PM) which S5 segment is linked to S4 segment by S4-S5 linker (119). After the neuronal depolarization, the S4 segment which has positive charge of arginine is activated by altering the electric field resulting in outward movement through the groove of S1-S3 segments to pull the S4-S5 linker that induced the conformation change of the intracellular side of S5-S6 segments to open the gate (119). Moreover, the pore is rapidly inactivated to Na^+ influx through isoleucine, phenylalanine, and methionine (IFM) motif of the interlinking Domain III and IV (DIII-DIV) that modulates the inactivation by moving to the intracellular pore for occlusion (120). Our findings showed that the height and overshoot of AP (AP_{height} and $AP_{overshoot}$) were reduced after pH change from 7.4 to 7.0.

These results are corresponded with the study of Vilin et al (121) demonstrated that low pH decreases AP_{height} and $AP_{overshoot}$ together with the time to peak of AP, which is faster compared with physiological pH. The reason is that the extracellular protons electrostatically bound to the carboxylated outer ring of channel pore and protonate some residues of amino acid. This condition causes Na_V channel block before IFM motif folding to the intracellular pore (121, 122). Therefore, the extracellular proton in pH 7.0 would directly block the pore of Na_V channels that leads to acceleration of the fast inactivation.

AHP is shaped by large (big) conductance calcium-activated potassium (BK_{Ca}) channel and small conductance calcium-activated potassium (SK_{Ca}) channel (123, 124). These channels are activated by the intracellular calcium (Ca^+) ion that are elevated via voltage-gated calcium channel (Ca_V). Then, Ca_V allows extracellular Ca^+ ions passing into neurons, and then inositol triphosphate (IP3) is activated that results in release of intracellular Ca^+ from endoplasmic reticulum to cytoplasm (125). The augment depolarization by increase of intracellular Ca^+ facilitates K^+ efflux that contributes to AHP. However, SK_{Ca} channel has more effect on AHP development compared with BK_{Ca} channel, whereas BK_{Ca} channel contributes in repolarization phase of AP (126). Our results showed that the depth of AHP (AHP_{depth}) was reduced in pH 7.0. This reduction may be modulated by the extracellular proton, which protonates histidine residues of outer pore of SK_{Ca} channels that results in the conformation change of pore to block K^+ efflux (127). Moreover, it was indicated that pro-inflammatory mediators including PGE_2 and serotonin can suppress the AHP amplitude (128, 129). Therefore, pH 7.0 may inhibit the AHP amplitude via SK_{Ca} channels. However, the duration of 50 % AHP_{depth} peak (AHP_{50}) was longer in pH 7.0 that may be caused from the long lasting open of potassium channels. It is known that potassium channels are opened as long as prolonged depolarization (105, 129). In our experiment, we changed physiological pH (pH 7.4) to pH 7.0 within 10 minutes, and then injected the depolarizing current to the neurons. The previous study of Waldmann et al (92) showed that prolonged pH change causes sustained currents indicating that some ASICs are opened as long as the activation by continuous low

pH. These may cause the neuronal depolarization, and may activate the other potassium channels.

Effect of pH 7.0 on the large-sized neurons

In contrast to the small-to-medium-sized neurons, the effect of pH 7.0 cannot change the neuronal excitability and AP shape of large-sized neurons.

As described above, the neuronal excitability and depolarization are regulated by ASICs, TASK-3, and TRESK. ASICs are expressed on the large-sized neurons, and low pH from 6.8 can activate these ASICs (11, 16, 18). Moreover, TASK-3 and TRESK are not expressed in the large-sized neurons (111, 130, 131). These evidences supports our results that pH 7.0 did not alter the neuronal excitability of large-sized neurons. The reason is that extracellular proton cannot activate ASICs on large-sized neurons, thus there are not any Na^+ influxes and K^+ accommodation inside neurons and then neurons are not depolarized. Moreover, our results also showed that AP shapes did not change in pH 7.0, because neuronal excitability was not altered.

Effect of CGRP in modulating pH 7.0 on the small-to-medium-sized neurons

In our experiment, pH 7.0 plus CGRP altered the excitability of small-to-medium-sized neurons that RMP was more negative. The AP shape was also changed that AP_{height} and $AP_{overshoot}$ were decreased, while rising time of AP (AP_{RT}) was longer than control. Interestingly, AHP_{depth} was increased. These results may be the secondary effect of CGRP that CGRP activates its receptor on satellite glia cells (SGCs) that released the pro-inflammatory mediators and activates the small-to-medium-sized neurons (22, 23, 132). The reason is that our primary culture was mixed-culture that consists of small to large diameter neurons and non-neuronal cells, including

SGCs. Moreover, our results in this condition were controversial with pH 7.0 condition, excepting AP_{height} and $AP_{overshoot}$.

As described above, RMP is modulated by the extracellular proton via ASICs activation that results in TASK-3 and TRESK inhibition. Our results demonstrated that RMP shifted to more negative when TG neurons were treated with CGRP in pH 7.0 condition. These results would possibly be affected by the pro-inflammatory cytokines that were released from SGCs. However, the mechanism of this modulation is unknown (22, 24).

Our results showed that AP_{height} and $AP_{overshoot}$ were reduced in the pH 7.0 plus CGRP condition. These reductions were similar to pH 7.0 condition that the extracellular proton blocked the pore of Na_V channels, which are direct effect of the extracellular proton (121). However, the rising time of AP (AP_{RT}) in our results was longer. This was because the secondary effect of CGRP may modulate the opening of gate of Na_V channels via unknown mechanism, while common Na_V channels was rapidly open in responding to depolarization (121).

AHP_{depth} is regulated by SK_{Ca} channels, and it is reduced by inhibition of the extracellular proton (127). However, in the pH 7.0 plus CGRP condition in our experiment, AHP_{depth} was increased that may be modulated by the secondary effect of CGRP that pro-inflammatory mediators may activate the small-to-medium-sized neurons to up-regulate the expression of SK_{Ca} channels or abolish the inhibition of the extracellular proton. However, the mechanism is unknown.

Thus, the secondary effect of CGRP via pro-inflammatory mediators of SGCs should be investigated in the future.

Effect of CGRP in modulating pH 7.0 on large-sized neurons

Our results indicated that CGRP modulated the excitability of large-sized neurons under pH 7.0, that the numbers of spike was increased and rheobase was reduced. These suggested that large-sized neurons expressed CGRP receptor (22, 25,

73). However, pH 7.0 cannot activate ASICs on the large-sized neurons as described above. Thus, these alterations may be directly caused from the activation of CGRP on its receptor.

Rheobase is a threshold current which is injected to neurons by commanding current to evoke AP. If the neurons are depolarized, the current that injected to the neurons is weakened. The neurons are depolarized by positive charge inside. Our results showed that rheobase was reduced in pH 7.0 plus CGRP conditions. The reason is that the activation of CGRP receptor produces protein kinase A and C (PKA and PKC) via G-protein signaling, that phosphorylates voltage-gated sodium channels (Na_V), including $Na_V1.6$ and $Na_V1.8$ (133, 134). Both $Na_V1.6$ and $Na_V1.8$ are expressed on the large-sized neurons (135, 136). In addition to rheobase, our findings showed that the number of spikes was increased that is consistent with the reduction of rheobase in pH 7.0 plus CGRP conditions. These results suggested that CGRP may directly affect the large-sized neurons via phosphorylation of voltage-gated sodium channels (Na_V) causing Na^+ influx and then AP is evoked.

The mechanism of CGRP activity
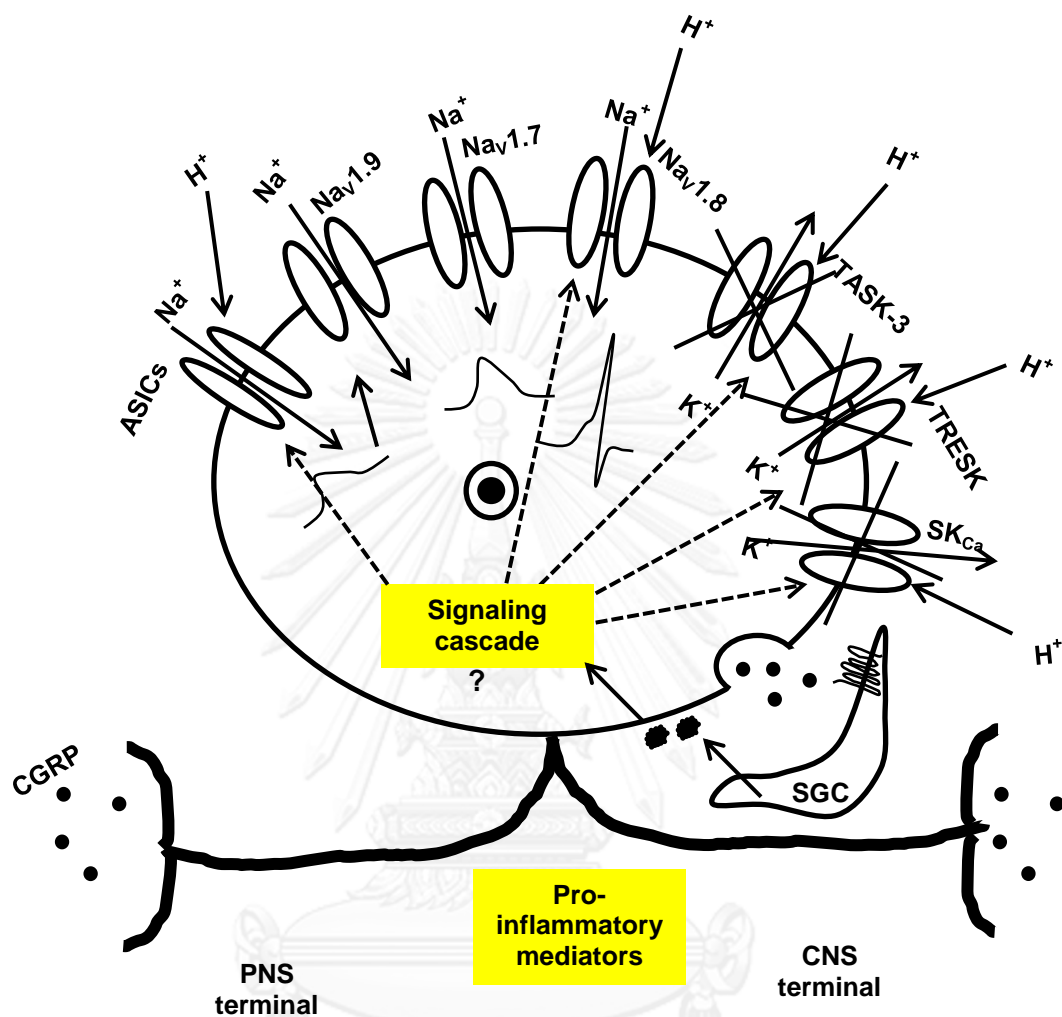
Figure 5.1 Illustration shows the modulation of CGRP on the excitability of the small-to-medium-sized neuron. CGRP may modulate the mechanism of the excitability via pro-inflammatory mediators from SGCs. The mechanism is unknown. There would be a signaling cascade that inhibits or activates or up-regulate the ion channels. These cascades are involved with the activation of the ASICs, that may inhibit the activation of TASK-3, TRESK, and SK_{Ca} (see dash arrow). These cascades may cause the hyperpolarization of neurons and enhances the depth of AHP.
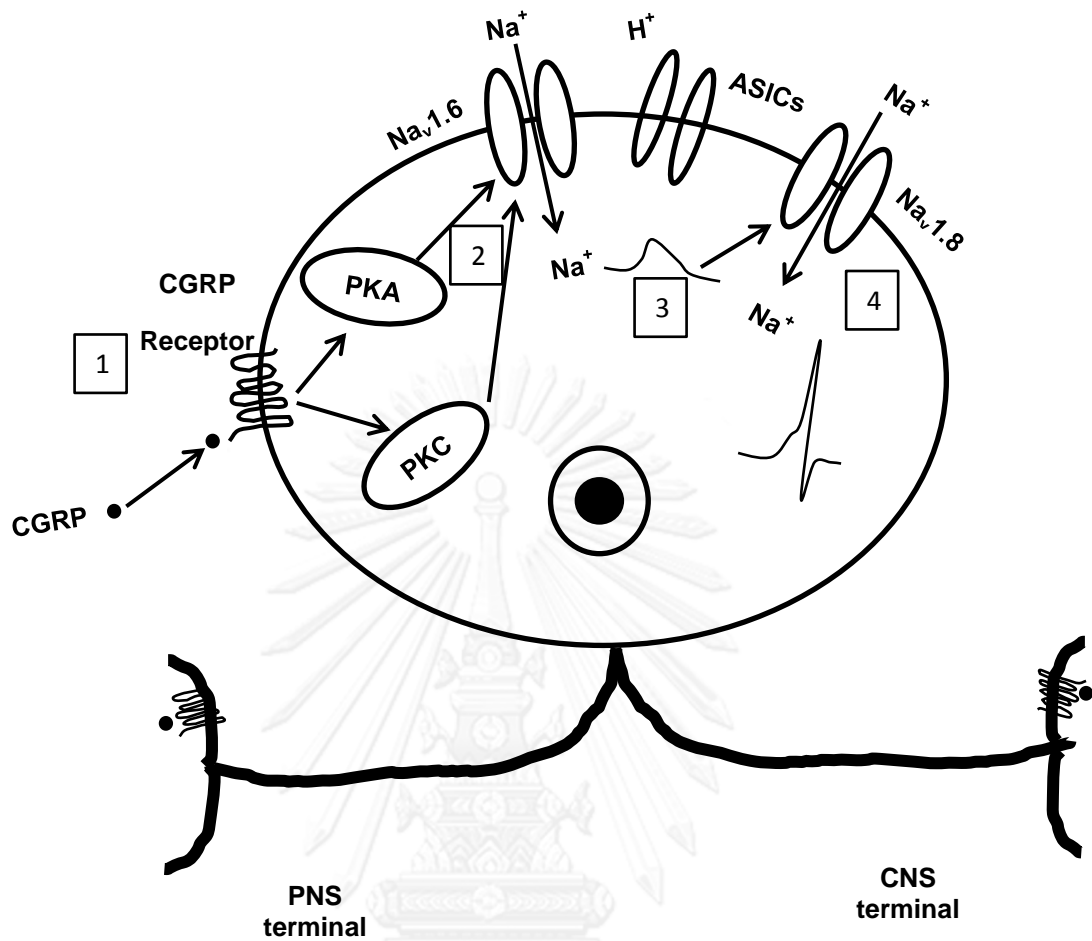
Figure 5.2 Illustration shows the modulation of CGRP on the excitability of large-sized neurons. The mechanism is initiated by CGRP as described below. First, CGRP activates its receptor causing up-regulation of PKA and PKC. Second, PKA and PKC may phosphorylate $Na_V1.6$ that leads to Na^+ influx. Third, Na^+ influx produces the neuronal depolarization. Fourth, the depolarization reaches the threshold of $Na_V1.8$ causing further Na^+ influx passing into neurons and producing AP.

Limitations

This study investigated in the condition of pH 7.4 versus pH 7.0 and pH 7.4 plus CGRP versus pH 7.0 plus CGRP. There is not any information about pH 7.4 versus pH 7.4 plus CGRP and pH 7.0 versus pH 7.0 plus CGRP. This limitation may make us difficult to interpret the results about the mechanism of the secondary effect of CGRP.

Future study

This experiment was performed under the current-clamp whole cell recording technique to study the role of pH 7.0 and the modulation of CGRP on pH 7.0 in the small-to-medium-sized and large-sized neurons. The molecular basis and the voltage-clamp whole cell recording technique are insufficiency. Hence, the expression, intracellular signaling pathways, and properties of individual ion channel should be investigated in the future study. Moreover, the further study should repeat experiments for investigating the condition pH 7.4 versus pH 7.4 plus CGRP and pH 7.0 versus pH 7.0 plus CGRP.

CHAPTER VI

CONCLUSION

The present study demonstrated that low pH (pH 7.0) alter the excitability and AP shapes of the small-to-medium-sized neurons via ASICs and other ion channels, while low pH did not alter the properties of the large-sized neurons. Moreover, CGRP has an effect on the properties of the large-sized neurons, whereas CGRP may modulate the effect of pH 7.0 on the small-to-medium-sized neurons via activation of the SGCs that may be the secondary effect of CGRP. However, the mechanism of the secondary effect of CGRP is unknown. These results indicated that CGRP has a direct effect on the large-sized neurons, while performed indirect effect on ASICs and other ion channels of the small-to-medium-sized neurons via the activation of the SGCs.

REFERENCES

1. Steen KH, Issberner U, Reeh PW. Pain due to experimental acidosis in human skin: evidence for non-adapting nociceptor excitation. Neuroscience letters. 1995;199(1):29-32.

2. Bender SD. Temporomandibular disorders, facial pain, and headaches. Headache. 2012;52 Suppl 1:22-5.

3. Steen KH, Reeh PW, Anton F, Handwerker HO. Protons selectively induce lasting excitation and sensitization to mechanical stimulation of nociceptors in rat skin, in vitro. The Journal of neuroscience : the official journal of the Society for Neuroscience. 1992;12(1):86-95.

4. Krishtal OA, Pidoplichko VI. A "receptor" for protons in small neurons of trigeminal ganglia: possible role in nociception. Neuroscience letters. 1981;24(3):243-6.

5. Cortright DN, Crandall M, Sanchez JF, Zou T, Krause JE, White G. The tissue distribution and functional characterization of human VR1. Biochemical and biophysical research communications. 2001;281(5):1183-9.

6. Ugawa S, Ueda T, Ishida Y, Nishigaki M, Shibata Y, Shimada S. Amiloride-blockable acid-sensing ion channels are leading acid sensors expressed in human nociceptors. The Journal of clinical investigation. 2002;110(8):1185-90.

7. Gonzales EB, Kawate T, Gouaux E. Pore architecture and ion sites in acid-sensing ion channels and P2X receptors. Nature. 2009;460(7255):599-604.

8. Lingueglia E. Acid-sensing ion channels in sensory perception. The Journal of biological chemistry. 2007;282(24):17325-9.

9. Chen CC, England S, Akopian AN, Wood JN. A sensory neuron-specific, proton-gated ion channel. Proceedings of the National Academy of Sciences of the United States of America. 1998;95(17):10240-5.

10. Ichikawa H, Sugimoto T. The co-expression of ASIC3 with calcitonin gene-related peptide and parvalbumin in the rat trigeminal ganglion. Brain research. 2002;943(2):287-91.

11. Molliver DC, Immke DC, Fierro L, Pare M, Rice FL, McCleskey EW. ASIC3, an acid-sensing ion channel, is expressed in metaboreceptive sensory neurons. Molecular pain. 2005;1:35.

12. Woolf CJ, Ma Q. Nociceptors--noxious stimulus detectors. Neuron. 2007;55(3):353-64.

13.   Sutherland SP, Benson CJ, Adelman JP, McCleskey EW. Acid-sensing ion channel 3 matches the acid-gated current in cardiac ischemia-sensing neurons. Proceedings of the National Academy of Sciences of the United States of America. 2001;98(2):711-6.

14.   Gu Q, Lee LY. Characterization of acid signaling in rat vagal pulmonary sensory neurons. American journal of physiology Lung cellular and molecular physiology. 2006;291(1):L58-65.

15.   Yan J, Edelmayer RM, Wei X, De Felice M, Porreca F, Dussor G. Dural afferents express acid-sensing ion channels: a role for decreased meningeal pH in migraine headache. Pain. 2011;152(1):106-13.

16.   Liu L, Simon SA. Capsaicin, acid and heat-evoked currents in rat trigeminal ganglion neurons: relationship to functional VR1 receptors. Physiology & behavior. 2000;69(3):363-78.

17.   Ichikawa H, Sugimoto T. VR1-immunoreactive primary sensory neurons in the rat trigeminal ganglion. Brain research. 2001;890(1):184-8.

18.   Connor M, Naves LA, McCleskey EW. Contrasting phenotypes of putative proprioceptive and nociceptive trigeminal neurons innervating jaw muscle in rat. Molecular pain. 2005;1:31.

19.   Fabbretti E, D'Arco M, Fabbro A, Simonetti M, Nistri A, Giniatullin R. Delayed upregulation of ATP P2X3 receptors of trigeminal sensory neurons by calcitonin gene-related peptide. The Journal of neuroscience : the official journal of the Society for Neuroscience. 2006;26(23):6163-71.

20.   Chatchaisak D, Srikiatkhachorn A, Maneesri-le Grand S, Govitrapong P, Chetsawang B. The role of calcitonin gene-related peptide on the increase in transient receptor potential vanilloid-1 levels in trigeminal ganglion and trigeminal nucleus caudalis activation of rat. Journal of chemical neuroanatomy. 2013;47:50-6.

21.   Durham PL, Masterson CG. Two mechanisms involved in trigeminal CGRP release: implications for migraine treatment. Headache. 2013;53(1):67-80.

22.   Eftekhari S, Edvinsson L. Possible sites of action of the new calcitonin gene-related peptide receptor antagonists. Therapeutic advances in neurological disorders. 2010;3(6):369-78.

23.   Kristiansen KA, Edvinsson L. Neurogenic inflammation: a study of rat trigeminal ganglion. The journal of headache and pain. 2010;11(6):485-95.

24.   Capuano A, De Corato A, Lisi L, Tringali G, Navarra P, Dello Russo C. Proinflammatory-activated trigeminal satellite cells promote neuronal sensitization: relevance for migraine pathology. Molecular pain. 2009;5:43.

25.	Eftekhari S, Warfvinge K, Blixt FW, Edvinsson L. Differentiation of nerve fibers storing CGRP and CGRP receptors in the peripheral trigeminovascular system. The journal of pain : official journal of the American Pain Society. 2013;14(11):1289-303.

26.	Ziyal IM, Sekhar LN, Ozgen T, Soylemezoglu F, Alper M, Beser M. The trigeminal nerve and ganglion: an anatomical, histological, and radiological study addressing the transtrigeminal approach. Surgical neurology. 2004;61(6):564-73; discussion 73-4.

27.	Bogduk N. Anatomy and physiology of headache. Biomedicine & pharmacotherapy = Biomedecine & pharmacotherapie. 1995;49(10):435-45.

28.	Andres KH, Von During M, Muszynski K, Schmidt RF. Nerve fibers and their terminals of the dura mater encephali of the rat. Anat Embryol. 1987;175:289-301.

29.	Krastev D, Paloff A, Hinova-Palova D, Apostolov A, Ovtscharoff W. Light-microscopic structure of trigeminal ganglion in humans. JIMAB Book. 2007;1:111-3.

30.	Krastev D. Satellite cells of trigeminal ganglion. JIMAB Book 2007;13:122-4.

31.	Kai-Kai MA. Cytochemistry of the trigeminal and dorsal root ganglia and spinal cord of the rat. Comparative biochemistry and physiology A, Comparative physiology. 1989;93(1):183-93.

32.	Ma QP, Hill R, Sirinathsinghji D. Colocalization of CGRP with 5-HT1B/1D receptors and substance P in trigeminal ganglion neurons in rats. The European journal of neuroscience. 2001;13(11):2099-104.

33.	Lazarov NE. Comparative analysis of the chemical neuroanatomy of the mammalian trigeminal ganglion and mesencephalic trigeminal nucleus. Progress in neurobiology. 2002;66(1):19-59.

34.	Julius D, Basbaum AI. Molecular mechanisms of nociception. Nature. 2001;413(6852):203-10.

35.	Kashiba H, Uchida Y, Senba E. Difference in binding by isolectin B4 to trkA and c-ret mRNA-expressing neurons in rat sensory ganglia. Brain research Molecular brain research. 2001;95(1-2):18-26.

36.	Price TJ, Flores CM. Critical evaluation of the colocalization between calcitonin gene-related peptide, substance P, transient receptor potential vanilloid subfamily type 1 immunoreactivities, and isolectin B4 binding in primary afferent neurons of the rat and mouse. The journal of pain : official journal of the American Pain Society. 2007;8(3):263-72.

37.	Weidner C, Schmelz M, Schmidt R, Hansson B, Handwerker HO, Torebjork HE. Functional attributes discriminating mechano-insensitive and mechano-responsive C

nociceptors in human skin. The Journal of neuroscience : the official journal of the Society for Neuroscience. 1999;19(22):10184-90.

38.   Price DD. Psychological and neural mechanisms of the affective dimension of pain. Science. 2000;288(5472):1769-72.

39.   Bessou P, Perl ER. Response of cutaneous sensory units with unmyelinated fibers to noxious stimuli. Journal of neurophysiology. 1969;32(6):1025-43.

40.   Woolf CJ, Costigan M. Transcriptional and posttranslational plasticity and the generation of inflammatory pain. Proceedings of the National Academy of Sciences of the United States of America. 1999;96(14):7723-30.

41.   Hu WP, Li XM, Wu JL, Zheng M, Li ZW. Bradykinin potentiates 5-HT3 receptor-mediated current in rat trigeminal ganglion neurons. Acta pharmacologica Sinica. 2005;26(4):428-34.

42.   Bellamy J, Bowen EJ, Russo AF, Durham PL. Nitric oxide regulation of calcitonin gene-related peptide gene expression in rat trigeminal ganglia neurons. The European journal of neuroscience. 2006;23(8):2057-66.

43.   Kadoi J, Takeda M, Matsumoto S. Prostaglandin E2 potentiates the excitability of small diameter trigeminal root ganglion neurons projecting onto the superficial layer of the cervical dorsal horn in rats. Experimental brain research Experimentelle Hirnforschung Experimentation cerebrale. 2007;176(2):227-36.

44.   Giniatullin R, Nistri A, Fabbretti E. Molecular mechanisms of sensitization of pain-transducing P2X3 receptors by the migraine mediators CGRP and NGF. Molecular neurobiology. 2008;37(1):83-90.

45.   Iadecola C. From CSD to headache: a long and winding road. Nature medicine. 2002;8(2):110-2.

46.   Gursoy-Ozdemir Y, Qiu J, Matsuoka N, Bolay H, Bermpohl D, Jin H, et al. Cortical spreading depression activates and upregulates MMP-9. The Journal of clinical investigation. 2004;113(10):1447-55.

47.   Reichling DB, Green PG, Levine JD. The fundamental unit of pain is the cell. Pain. 2013;154 Suppl 1:S2-9.

48.   Goadsby PJ, Hoskin KL. The distribution of trigeminovascular afferents in the nonhuman primate brain Macaca nemestrina: a c-fos immunocytochemical study. Journal of anatomy. 1997;190 (Pt 3):367-75.

49.   Bereiter DA, Hirata H, Hu JW. Trigeminal subnucleus caudalis: beyond homologies with the spinal dorsal horn. Pain. 2000;88(3):221-4.

50.   Goadsby PJ, Classey JD. Glutamatergic transmission in the trigeminal nucleus assessed with local blood flow. Brain research. 2000;875(1-2):119-24.

51.   Broton JG, Hu JW, Sessle BJ. Effects of temporomandibular joint stimulation on nociceptive and nonnociceptive neurons of the cat's trigeminal subnucleus caudalis (medullary dorsal horn). Journal of neurophysiology. 1988;59(5):1575-89.

52.   Storer RJ, Akerman S, Goadsby PJ. GABA receptors modulate trigeminovascular nociceptive neurotransmission in the trigeminocervical complex. British journal of pharmacology. 2001;134(4):896-904.

53.   Akerman S, Holland PR, Goadsby PJ. Diencephalic and brainstem mechanisms in migraine. Nature reviews Neuroscience. 2011;12(10):570-84.

54.   Pietrobon D, Striessnig J. Neurobiology of migraine. Nature reviews Neuroscience. 2003;4(5):386-98.

55.   Moskowitz MA, Cutrer FM. SUMATRIPTAN: a receptor-targeted treatment for migraine. Annual review of medicine. 1993;44:145-54.

56.   Longoni M, Ferrarese C. Inflammation and excitotoxicity: role in migraine pathogenesis. Neurological sciences : official journal of the Italian Neurological Society and of the Italian Society of Clinical Neurophysiology. 2006;27 Suppl 2:S107-10.

57.   Chiu IM, von Hehn CA, Woolf CJ. Neurogenic inflammation and the peripheral nervous system in host defense and immunopathology. Nature neuroscience. 2012;15(8):1063-7.

58.   McCulloch J, Uddman R, Kingman TA, Edvinsson L. Calcitonin gene-related peptide: functional role in cerebrovascular regulation. Proceedings of the National Academy of Sciences of the United States of America. 1986;83(15):5731-5.

59.   Edvinsson L, Ekman R, Jansen I, McCulloch J, Uddman R. Calcitonin gene-related peptide and cerebral blood vessels: distribution and vasomotor effects. Journal of cerebral blood flow and metabolism : official journal of the International Society of Cerebral Blood Flow and Metabolism. 1987;7(6):720-8.

60.   Thalakoti S, Patil VV, Damodaram S, Vause CV, Langford LE, Freeman SE, et al. Neuron-glia signaling in trigeminal ganglion: implications for migraine pathology. Headache. 2007;47(7):1008-23; discussion 24-5.

61.   Ren K, Dubner R. Interactions between the immune and nervous systems in pain. Nature medicine. 2010;16(11):1267-76.

62.   Levy D, Burstein R, Strassman AM. Mast cell involvement in the pathophysiology of migraine headache: A hypothesis. Headache. 2006;46 Suppl 1:S13-8.

63.   Alhelal MA, Palaska I, Panagiotidou S, Letourneau R, Theoharides TC. Trigeminal nerve stimulation triggers oral mast cell activation and vascular

permeability. Annals of allergy, asthma & immunology : official publication of the American College of Allergy, Asthma, & Immunology. 2014;112(1):40-5.

64.   Yan J, Wei X, Bischoff C, Edelmayer RM, Dussor G. pH-Evoked Dural Afferent Signaling Is Mediated by ASIC3 and Is Sensitized by Mast Cell Mediators. Headache. 2013;53(8):1250-61.

65.   Levy D, Burstein R, Kainz V, Jakubowski M, Strassman AM. Mast cell degranulation activates a pain pathway underlying migraine headache. Pain. 2007;130(1-2):166-76.

66.   Durham PL. Calcitonin gene-related peptide (CGRP) and migraine. Headache. 2006;46 Suppl 1:S3-8.

67.   Poyner DR, Sexton PM, Marshall I, Smith DM, Quirion R, Born W, et al. International Union of Pharmacology. XXXII. The mammalian calcitonin gene-related peptides, adrenomedullin, amylin, and calcitonin receptors. Pharmacological reviews. 2002;54(2):233-46.

68.   McLatchie LM, Fraser NJ, Main MJ, Wise A, Brown J, Thompson N, et al. RAMPs regulate the transport and ligand specificity of the calcitonin-receptor-like receptor. Nature. 1998;393(6683):333-9.

69.   Evans BN, Rosenblatt MI, Mnayer LO, Oliver KR, Dickerson IM. CGRP-RCP, a novel protein required for signal transduction at calcitonin gene-related peptide and adrenomedullin receptors. The Journal of biological chemistry. 2000;275(40):31438-43.

70.   Springer J, Geppetti P, Fischer A, Groneberg DA. Calcitonin gene-related peptide as inflammatory mediator. Pulmonary pharmacology & therapeutics. 2003;16(3):121-30.

71.   Arulmani U, Maassenvandenbrink A, Villalon CM, Saxena PR. Calcitonin gene-related peptide and its role in migraine pathophysiology. European journal of pharmacology. 2004;500(1-3):315-30.

72.   Lennerz JK, Ruhle V, Ceppa EP, Neuhuber WL, Bunnett NW, Grady EF, et al. Calcitonin receptor-like receptor (CLR), receptor activity-modifying protein 1 (RAMP1), and calcitonin gene-related peptide (CGRP) immunoreactivity in the rat trigeminovascular system: differences between peripheral and central CGRP receptor distribution. The Journal of comparative neurology. 2008;507(3):1277-99.

73.   Eftekhari S, Salvatore CA, Calamari A, Kane SA, Tajti J, Edvinsson L. Differential distribution of calcitonin gene-related peptide and its receptor components in the human trigeminal ganglion. Neuroscience. 2010;169(2):683-96.

74.   Eftekhari S, Edvinsson L. Calcitonin gene-related peptide (CGRP) and its receptor components in human and rat spinal trigeminal nucleus and spinal cord at C1-level. BMC neuroscience. 2011;12:112.

75.   Durham PL, Cady R, Cady R. Regulation of calcitonin gene-related peptide secretion from trigeminal nerve cells by botulinum toxin type A: implications for migraine therapy. Headache. 2004;44(1):35-42; discussion -3.

76.   Messlinger K, Lennerz JK, Eberhardt M, Fischer MJ. CGRP and NO in the trigeminal system: mechanisms and role in headache generation. Headache. 2012;52(9):1411-27.

77.   Damodaram S, Thalakoti S, Freeman SE, Garrett FG, Durham PL. Tonabersat inhibits trigeminal ganglion neuronal-satellite glial cell signaling. Headache. 2009;49(1):5-20.

78.   Edvinsson L. CGRP-receptor antagonism in migraine treatment. Lancet. 2008;372(9656):2089-90.

79.   Zhang Z, Winborn CS, Marquez de Prado B, Russo AF. Sensitization of calcitonin gene-related peptide receptors by receptor activity-modifying protein-1 in the trigeminal ganglion. The Journal of neuroscience : the official journal of the Society for Neuroscience. 2007;27(10):2693-703.

80.   Simonetti M, Giniatullin R, Fabbretti E. Mechanisms mediating the enhanced gene transcription of P2X3 receptor by calcitonin gene-related peptide in trigeminal sensory neurons. The Journal of biological chemistry. 2008;283(27):18743-52.

81.   Drissi H, Lasmoles F, Le Mellay V, Marie PJ, Lieberherr M. Activation of phospholipase C-beta1 via Galphaq/11 during calcium mobilization by calcitonin gene-related peptide. The Journal of biological chemistry. 1998;273(32):20168-74.

82.   Walker CS, Conner AC, Poyner DR, Hay DL. Regulation of signal transduction by calcitonin gene-related peptide receptors. Trends in pharmacological sciences. 2010;31(10):476-83.

83.   Vause CV, Durham PL. Calcitonin gene-related peptide differentially regulates gene and protein expression in trigeminal glia cells: findings from array analysis. Neuroscience letters. 2010;473(3):163-7.

84.   Cady RJ, Glenn JR, Smith KM, Durham PL. Calcitonin gene-related peptide promotes cellular changes in trigeminal neurons and glia implicated in peripheral and central sensitization. Molecular pain. 2011;7:94.

85.   Waldmann R, Champigny G, Bassilana F, Heurteaux C, Lazdunski M. A proton-gated cation channel involved in acid-sensing. Nature. 1997;386(6621):173-7.

86.   Jasti J, Furukawa H, Gonzales EB, Gouaux E. Structure of acid-sensing ion channel 1 at 1.9 A resolution and low pH. Nature. 2007;449(7160):316-23.

87.   Garcia-Anoveros J, Derfler B, Neville-Golden J, Hyman BT, Corey DP. BNaC1 and BNaC2 constitute a new family of human neuronal sodium channels related to degenerins and epithelial sodium channels. Proceedings of the National Academy of Sciences of the United States of America. 1997;94(4):1459-64.

88.   Bassler EL, Ngo-Anh TJ, Geisler HS, Ruppersberg JP, Grunder S. Molecular and functional characterization of acid-sensing ion channel (ASIC) 1b. The Journal of biological chemistry. 2001;276(36):33782-7.

89.   Waldmann R, Champigny G, Voilley N, Lauritzen I, Lazdunski M. The mammalian degenerin MDEG, an amiloride-sensitive cation channel activated by mutations causing neurodegeneration in Caenorhabditis elegans. The Journal of biological chemistry. 1996;271(18):10433-6.

90.   Bassilana F, Champigny G, Waldmann R, de Weille JR, Heurteaux C, Lazdunski M. The acid-sensitive ionic channel subunit ASIC and the mammalian degenerin MDEG form a heteromultimeric H+-gated Na+ channel with novel properties. The Journal of biological chemistry. 1997;272(46):28819-22.

91.   Lingueglia E, de Weille JR, Bassilana F, Heurteaux C, Sakai H, Waldmann R, et al. A modulatory subunit of acid sensing ion channels in brain and dorsal root ganglion cells. The Journal of biological chemistry. 1997;272(47):29778-83.

92.   Waldmann R, Bassilana F, de Weille J, Champigny G, Heurteaux C, Lazdunski M. Molecular cloning of a non-inactivating proton-gated Na+ channel specific for sensory neurons. The Journal of biological chemistry. 1997;272(34):20975-8.

93.   Akopian AN, Chen CC, Ding Y, Cesare P, Wood JN. A new member of the acid-sensing ion channel family. Neuroreport. 2000;11(10):2217-22.

94.   Olson TH, Riedl MS, Vulchanova L, Ortiz-Gonzalez XR, Elde R. An acid sensing ion channel (ASIC) localizes to small primary afferent neurons in rats. Neuroreport. 1998;9(6):1109-13.

95.   Waldmann R, Lazdunski M. H(+)-gated cation channels: neuronal acid sensors in the NaC/DEG family of ion channels. Current opinion in neurobiology. 1998;8(3):418-24.

96.   Benson CJ, Xie J, Wemmie JA, Price MP, Henss JM, Welsh MJ, et al. Heteromultimers of DEG/ENaC subunits form H+-gated channels in mouse sensory neurons. Proceedings of the National Academy of Sciences of the United States of America. 2002;99(4):2338-43.

97.   Hesselager M, Timmermann DB, Ahring PK. pH Dependency and desensitization kinetics of heterologously expressed combinations of acid-sensing ion channel subunits. The Journal of biological chemistry. 2004;279(12):11006-15.

98.   Deval E, Gasull X, Noel J, Salinas M, Baron A, Diochot S, et al. Acid-sensing ion channels (ASICs): pharmacology and implication in pain. Pharmacology & therapeutics. 2010;128(3):549-58.

99.   Allard M, Rousselot P, Lombard MC, Theodosis DT. Evidence for neuropeptide FF (FLFQRFamide) in rat dorsal root ganglia. Peptides. 1999;20(3):327-33.

100.   Askwith CC, Cheng C, Ikuma M, Benson C, Price MP, Welsh MJ. Neuropeptide FF and FMRFamide potentiate acid-evoked currents from sensory neurons and proton-gated DEG/ENaC channels. Neuron. 2000;26(1):133-41.

101.   Deval E, Baron A, Lingueglia E, Mazarguil H, Zajac JM, Lazdunski M. Effects of neuropeptide SF and related peptides on acid sensing ion channel 3 and sensory neuron excitability. Neuropharmacology. 2003;44(5):662-71.

102.   Xie J, Price MP, Wemmie JA, Askwith CC, Welsh MJ. ASIC3 and ASIC1 mediate FMRFamide-related peptide enhancement of H+-gated currents in cultured dorsal root ganglion neurons. Journal of neurophysiology. 2003;89(5):2459-65.

103.   Mamet J, Baron A, Lazdunski M, Voilley N. Proinflammatory mediators, stimulators of sensory neuron excitability via the expression of acid-sensing ion channels. The Journal of neuroscience : the official journal of the Society for Neuroscience. 2002;22(24):10662-70.

104.   Malin SA, Davis BM, Molliver DC. Production of dissociated sensory neuron cultures and considerations for their use in studying neuronal function and plasticity. Nature protocols. 2007;2(1):152-60.

105.   Catacuzzeno L, Fioretti B, Pietrobon D, Franciolini F. The differential expression of low-threshold K+ currents generates distinct firing patterns in different subtypes of adult mouse trigeminal ganglion neurones. The Journal of physiology. 2008;586(Pt 21):5101-18.

106.   Cummins TR, Dib-Hajj SD, Black JA, Akopian AN, Wood JN, Waxman SG. A novel persistent tetrodotoxin-resistant sodium current in SNS-null and wild-type small primary sensory neurons. The Journal of neuroscience : the official journal of the Society for Neuroscience. 1999;19(24):Rc43.

107.   Goldstein SA, Bockenhauer D, O'Kelly I, Zilberberg N. Potassium leak channels and the KCNK family of two-P-domain subunits. Nature reviews Neuroscience. 2001;2(3):175-84.

108.   Brown DA, Passmore GM. Neural KCNQ (Kv7) channels. British journal of pharmacology. 2009;156(8):1185-95.

109.   Rajan S, Wischmeyer E, Xin Liu G, Preisig-Muller R, Daut J, Karschin A, et al. TASK-3, a novel tandem pore domain acid-sensitive K+ channel. An extracellular histiding as pH sensor. The Journal of biological chemistry. 2000;275(22):16650-7.

110.   Keshavaprasad B, Liu C, Au JD, Kindler CH, Cotten JF, Yost CS. Species-specific differences in response to anesthetics and other modulators by the K2P channel TRESK. Anesthesia and analgesia. 2005;101(4):1042-9, table of contents.

111.   Bautista DM, Sigal YM, Milstein AD, Garrison JL, Zorn JA, Tsuruda PR, et al. Pungent agents from Szechuan peppers excite sensory neurons by inhibiting two-pore potassium channels. Nature neuroscience. 2008;11(7):772-9.

112.   Rush AM, Dib-Hajj SD, Liu S, Cummins TR, Black JA, Waxman SG. A single sodium channel mutation produces hyper- or hypoexcitability in different types of neurons. Proceedings of the National Academy of Sciences of the United States of America. 2006;103(21):8245-50.

113.   Ostman JA, Nassar MA, Wood JN, Baker MD. GTP up-regulated persistent Na+ current and enhanced nociceptor excitability require NaV1.9. The Journal of physiology. 2008;586(4):1077-87.

114.   England S, Bevan S, Docherty RJ. PGE2 modulates the tetrodotoxin-resistant sodium current in neonatal rat dorsal root ganglion neurones via the cyclic AMP-protein kinase A cascade. The Journal of physiology. 1996;495 (Pt 2):429-40.

115.   Rush AM, Waxman SG. PGE2 increases the tetrodotoxin-resistant Nav1.9 sodium current in mouse DRG neurons via G-proteins. Brain research. 2004;1023(2):264-71.

116.   Baker MD, Chandra SY, Ding Y, Waxman SG, Wood JN. GTP-induced tetrodotoxin-resistant Na+ current regulates excitability in mouse and rat small diameter sensory neurones. The Journal of physiology. 2003;548(Pt 2):373-82.

117.   Waxman SG, Estacion M. Nav1.9, G-proteins, and nociceptors. The Journal of physiology. 2008;586(4):917-8.

118.   Dib-Hajj SD, Yang Y, Black JA, Waxman SG. The Na(V)1.7 sodium channel: from molecule to man. Nature reviews Neuroscience. 2013;14(1):49-62.

119.   Yarov-Yarovoy V, DeCaen PG, Westenbroek RE, Pan CY, Scheuer T, Baker D, et al. Structural basis for gating charge movement in the voltage sensor of a sodium channel. Proceedings of the National Academy of Sciences of the United States of America. 2012;109(2):E93-102.

120.   West JW, Patton DE, Scheuer T, Wang Y, Goldin AL, Catterall WA. A cluster of hydrophobic amino acid residues required for fast Na(+)-channel inactivation. Proceedings of the National Academy of Sciences of the United States of America. 1992;89(22):10910-4.

121.   Vilin YY, Peters CH, Ruben PC. Acidosis differentially modulates inactivation in na(v)1.2, na(v)1.4, and na(v)1.5 channels. Frontiers in pharmacology. 2012;3:109.

122.   Khan A, Romantseva L, Lam A, Lipkind G, Fozzard HA. Role of outer ring carboxylates of the rat skeletal muscle sodium channel pore in proton block. The Journal of physiology. 2002;543(Pt 1):71-84.

123.   Wei AD, Gutman GA, Aldrich R, Chandy KG, Grissmer S, Wulff H. International Union of Pharmacology. LII. Nomenclature and molecular relationships of calcium-activated potassium channels. Pharmacological reviews. 2005;57(4):463-72.

124.   Stemkowski PL, Smith PA. Sensory neurons, ion channels, inflammation and the onset of neuropathic pain. The Canadian journal of neurological sciences Le journal canadien des sciences neurologiques. 2012;39(4):416-35.

125.   Adelman JP, Maylie J, Sah P. Small-conductance Ca2+-activated K+ channels: form and function. Annual review of physiology. 2012;74:245-69.

126.   Sah P. Ca(2+)-activated K+ currents in neurones: types, physiological roles and modulation. Trends in neurosciences. 1996;19(4):150-4.

127.   Goodchild SJ, Lamy C, Seutin V, Marrion NV. Inhibition of K(Ca)2.2 and K(Ca)2.3 channel currents by protonation of outer pore histidine residues. The Journal of general physiology. 2009;134(4):295-308.

128.   Catarsi S, Brunelli M. Serotonin depresses the after-hyperpolarization through the inhibition of the Na+/K+ electrogenic pump in T sensory neurones of the leech. The Journal of experimental biology. 1991;155:261-73.

129.   Gold MS, Shuster MJ, Levine JD. Role of a Ca(2+)-dependent slow afterhyperpolarization in prostaglandin E2-induced sensitization of cultured rat sensory neurons. Neuroscience letters. 1996;205(3):161-4.

130.   Lafreniere RG, Cader MZ, Poulin JF, Andres-Enguix I, Simoneau M, Gupta N, et al. A dominant-negative mutation in the TRESK potassium channel is linked to familial migraine with aura. Nature medicine. 2010;16(10):1157-60.

131.   Pollema-Mays SL, Centeno MV, Ashford CJ, Apkarian AV, Martina M. Expression of background potassium channels in rat DRG is cell-specific and down-regulated in a neuropathic pain model. Molecular and cellular neurosciences. 2013;57:1-9.

132.   Ceruti S, Villa G, Fumagalli M, Colombo L, Magni G, Zanardelli M, et al. Calcitonin gene-related peptide-mediated enhancement of purinergic neuron/glia

communication by the algogenic factor bradykinin in mouse trigeminal ganglia from wild-type and R192Q Cav2.1 Knock-in mice: implications for basic mechanisms of migraine pain. The Journal of neuroscience : the official journal of the Society for Neuroscience. 2011;31(10):3638-49.

133.   Sun RQ, Tu YJ, Lawand NB, Yan JY, Lin Q, Willis WD. Calcitonin gene-related peptide receptor activation produces PKA- and PKC-dependent mechanical hyperalgesia and central sensitization. Journal of neurophysiology. 2004;92(5):2859-66.

134.   Natura G, von Banchet GS, Schaible HG. Calcitonin gene-related peptide enhances TTX-resistant sodium currents in cultured dorsal root ganglion neurons from adult rats. Pain. 2005;116(3):194-204.

135.   Cummins TR, Dib-Hajj SD, Herzog RI, Waxman SG. Nav1.6 channels generate resurgent sodium currents in spinal sensory neurons. FEBS letters. 2005;579(10):2166-70.

136.   Ramachandra R, McGrew SY, Baxter JC, Howard JR, Elmslie KS. NaV1.8 channels are expressed in large, as well as small, diameter sensory afferent neurons. Channels (Austin). 2013;7(1):34-7.

VITA

Name	Mister Uggrit Junsre
Date of birth	August 30th, 1987
Place of birth	Buriram, Thailand
Education credential	Chulalongkorn University (2006-2009)
	Bachelor's degree of Science, Physical Therapy